



National Library
of Canada

Bibliothèque nationale
du Canada

Canadian Theses Service

Service des thèses canadiennes

Ottawa, Canada
K1A 0N4

NOTICE

The quality of this microform is heavily dependent upon the quality of the original thesis submitted for microfilming. Every effort has been made to ensure the highest quality of reproduction possible.

If pages are missing, contact the university which granted the degree.

Some pages may have indistinct print especially if the original pages were typed with a poor typewriter ribbon or if the university sent us an inferior photocopy.

Reproduction in full or in part of this microform is governed by the Canadian Copyright Act, R.S.C. 1970, c. C-30, and subsequent amendments.

AVIS

La qualité de cette microforme dépend grandement de la qualité de la thèse soumise au microfilmage. Nous avons tout fait pour assurer une qualité supérieure de reproduction.

S'il manque des pages, veuillez communiquer avec l'université qui a conféré le grade.

La qualité d'impression de certaines pages peut laisser à désirer, surtout si les pages originales ont été dactylographiées à l'aide d'un ruban usé ou si l'université nous a fait parvenir une photocopie de qualité inférieure.

La reproduction, même partielle, de cette microforme est soumise à la Loi canadienne sur le droit d'auteur, SRC 1970, c. C-30, et ses amendements subséquents.

University of Alberta

**The costs and benefits of large neuronal ensembles
and high firing rates for the transmission of
information in neuronal systems.**

By



Steven J. Vincent.

A Thesis

Submitted to the faculty of Graduate Studies and Research in
partial fulfilment of the requirements for the degree of
Master of Science

Department of Physiology.

Edmonton Alberta.

Fall 1990



National Library
of Canada

Bibliothèque nationale
du Canada

Canadian Theses Service Service des thèses canadiennes

Ottawa, Canada
K1A 0N4

The author has granted an irrevocable non-exclusive licence allowing the National Library of Canada to reproduce, loan, distribute or sell copies of his/her thesis by any means and in any form or format, making this thesis available to interested persons.

The author retains ownership of the copyright in his/her thesis. Neither the thesis nor substantial extracts from it may be printed or otherwise reproduced without his/her permission.

L'auteur a accordé une licence irrévocable et non exclusive permettant à la Bibliothèque nationale du Canada de reproduire, prêter, distribuer ou vendre des copies de sa thèse de quelque manière et sous quelque forme que ce soit pour mettre des exemplaires de cette thèse à la disposition des personnes intéressées.

L'auteur conserve la propriété du droit d'auteur qui protège sa thèse. Ni la thèse ni des extraits substantiels de celle-ci ne doivent être imprimés ou autrement reproduits sans son autorisation.

ISBN 0-315-65089-3



University of Alberta
Edmonton

Canada T6G 2S2

Division of Neuroscience
Faculty of Medicine

513 Heritage Medical Research Centre
Telephone (403) 492-5749

Steven Vincent

10 October 1990

Dear Sir

I hereby give permission to Mr. S. Vincent to reproduce, for his Masters Thesis, figure 7 from my 1967 paper "The information capacity of nerve cells using a frequency code." Biophysical Journal 7:797-826 .

Yours Sincerely

R.B. Stein

Dr. R. B. Stein

Director.

Division of Neuroscience

Professor of Physiology.

UNIVERSITY OF ALBERTA

RELEASE FORM

NAME OF AUTHOR: Steven John Vincent

TITLE OF THESIS: The costs and benefits of large neuronal ensembles and high firing rates for the transmission of information in neuronal systems

DEGREE: Master of Science

YEAR THIS DEGREE IS GRANTED: 1990

Permission is hereby granted to THE UNIVERSITY OF ALBERTA LIBRARY to reproduce single copies of this thesis and to lend or sell such copies for private, scholarly or scientific research purposes only.

The author reserves other publication rights, and neither the thesis nor extensive extracts from it may be printed or otherwise reproduced without the author's written permission



(Student's signature)

(Student's permanent address)

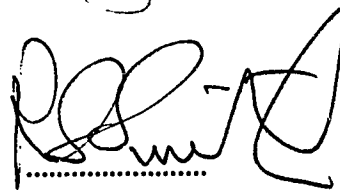
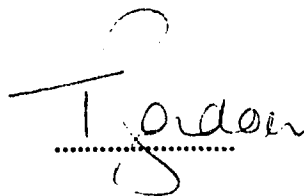
Date 10 October 1990

THE UNIVERSITY OF ALBERTA
FACULTY OF GRADUATE STUDIES AND RESEARCH

The undersigned certify that they have read, and recommended to the Faculty of Graduate Studies and Research for acceptance, a thesis entitled THE COSTS AND BENEFITS OF LARGE NEURONAL ENSEMBLES AND HIGH FIRING RATES FOR THE TRANSMISSION OF INFORMATION IN NEURONAL SYSTEMS submitted by Steven John Vincent in partial fulfilment of the requirements for the degree of Master of Science.



(Supervisor)



Date; *Oct. 9/90*

ABSTRACT

- 1 The costs and benefits associated with varying numbers of neurons transmitting information at varying firing frequencies were studied.
- 2 The limiting step for neuronal activity is the availability of transmitter in releasable form. Transmitter replacement is exceeded at quite moderate firing rates, though internal stores enable neurons to fire high frequency bursts.
- 3 The summated firing and post-synaptic action of discrete functional groups of neurons (Ia muscle spindle afferents) were studied. Ia firing profiles were either modeled, or collated from single fibre recordings supplied by Dr. M. Hulliger. Initially we characterised the range of Ia firing behaviour during ramp-and-hold stretches. The resulting cumulative probability curves were used to combine afferents into representative ensembles of differing size. These ensemble spike trains were then applied to a motoneuron model.
- 4 The low-pass filtering characteristics of the motoneuron model greatly attenuated the "noisiness" of the contributing ensembles. The larger the ensembles, the better the signal to noise ratio (SNR). There was broad agreement with Stein's (1967b) proposal that the information carried by a neuronal ensemble is: (information carried by one neuron) $\times \sqrt{\text{number of neurons}}$.

- 5 Surprisingly, SNR was not uniquely determined by net ensemble firing rate: SNR was higher for a small ensemble with a high mean rate than for a large ensemble with a low mean rate (same net firing rate). In a given ensemble the SNR improved with increasing net firing rate, regardless of whether this was produced by γ stimulation or stretch.
- 6 Static fusimotor (γ_s) stimulation improved SNR by increasing the mean firing rate ("bias"). This was costly, in that the total number of spikes over the whole displacement cycle was higher for γ_s action than for dynamic fusimotor (γ_d) action. γ_d action increased SNR (and cost) during lengthening because the mean carrier rates were greatly elevated. During shortening, γ_d action did not maintain Ia firing: no information was transmitted.
- 7 γ drive, by increasing Ia firing rates, can quadruple resolution at the motoneuron. It would require a 16 fold increase in afferent numbers to achieve this without γ action. We infer that fusimotor action maximises (SNR/costs) "when needed", by driving afferents to frequencies not sustainable indefinitely. This incurs metabolic debts which must be repaid.

ACKNOWLEDGEMENTS

I am grateful to Dr. Arthur Prochazka for the opportunity to do this degree and his help and assistance with the work.

I must also thank Dr. M. Hulliger who graciously provided me with the large database of afferent responses upon which much of this work has been based.

To Alison my thanks for her patience and continuing support during the long winters

TABLE OF CONTENTS

ABSTRACT	iv
ACKNOWLEDGEMENTS	vi
ABBREVIATIONS	xi
1 INTRODUCTION	1
1.1 The nature of neuronal information transmission	1
1.2 Comparison of PFM and binary information transmission systems.	2
1.3 Limitations on the conduction of action potentials	5
1.4 Costs of synaptic transmission.	8
1.5 Measures of information and estimations of resolution	13
1.6 Algebraic summation in motoneurons	16
1.7 Summary of aims of experiments.	17
2 METHODS	19
2.1 Acute recordings	19
2.1.1 Preparation	19
2.1.2 Selection of neurons	20
2.1.3 Recording of data	21
2.2 Synthetic firing profiles	21

2.3 Real unit firing profiles	24
2.3.1 Population distributions	24
2.3.2 Combination into populations	26
2.4 Construction of the motoneuron model.	27
2.4.1 Passage through the motoneuron model.	28
2.5 Quantitative analysis.	28
2.6 Pre-processing	29
2.6.1 MassAvg	30
2.6.2 Extract	31
3 RESULTS	32
3.1 Population distributions	32
3.2 Modeled units	41
3.2.1 Effects of inter-spike variability and population size.	41
3.3 Recorded primary muscle afferents	43
3.3.1 Single units	43
3.3.2 Ensembles of primary muscle afferents	43
4 DISCUSSION	48
4.1 Neuronal ensembles	48
4.2 Quantitative information on Ia afferent behaviour	50
4.3 Cumulative data enables the construction of typical populations ...	51
4.4 Dynamic components of response: signal or noise ?	53
4.5 Predictions from mathematical analysis	54

4.6	Smoothing effects of the motoneuron model.	57
4.7	The effects of synchronisation between muscle afferent discharges. .	58
4.8	Interspike variability.	59
4.9	Implications from modelled units	60
4.10	Implications from assembled populations	60
4.11	Effect of population size	61
4.12	Other target neurones	63
5 CONCLUSIONS		65
REFERENCES		67
Appendix: The MassAvg program		75

LIST OF FIGURES

1 Recovery of information from a frequency code using a low pass filter.	3
2 Cost of conducting action potentials.	7
3 Schematic representation of information capacity as a function of stimulus duration for a neuron, <u>a)</u> Discharging randomly with FM <u>b)</u> Regular discharge with FM <u>c)</u> binary pulse code <u>d)</u> interval code. From Stein 1967b	14
4 Schematic representation of the experimental setup.	22
5 Construction of ensemble responses.	25
6 The frequency distributions of Ia afferent populations at three positions in a ramp stretch.	33
7 Frequency of firing in Ia afferent populations during a ramp stretch.	34
8 The effects of fusimotor activity on the distribution of firing frequencies seen in Ia afferents during a ramp stretch.	35
9 The cumulative probability functions used to assemble typical populations.	37
10 Ensemble responses of 50 Ia afferents to a standard ramp and hold stretch.	38
11 The effects of interspike variability on the motoneuron model.	40
12 The signal to noise ratios of different sized populations of Ia afferents during a ramp stretch under different types of fusimotor drive.	42
13 Signal transmission by a Ia afferent to an α -motoneuron	44
14 Resolution of Ia ensemble responses	45
15 Signal to noise v mean afferent firing rate.	47

ABBREVIATIONS

γ_d	Dynamic fusimotor
γ_s	Static fusimotor
ACh	acetyl choline
CED	Cambridge Electronic Design
CM	cortico-motoneuron
DAC	Digital to analog converter
DI	Dynamic Index
DSCCT	dorso-spinocerebellar tract
emg	Electromyogram
EPP	End plate potential
EPSP	Excitatory post-synaptic potential
f-I	Frequency current relationship
Ia	Primary muscle spindle afferent
Ib	Golgi Tendon organ afferent
IPFM	impulse frequency modulation
ips	Impulses per second
IPSP	Inhibitory post-synaptic potential
pdf	Probability density function
PFM	Pulse frequency modulation
S.D.	Standard deviation
SNR	Signal to noise ratio (mean/ (2σ))

1 INTRODUCTION

1.1 The nature of neuronal information transmission.

Information in the nervous system is carried as impulses along nerve fibres and the numbers of these impulses can vary from less than 10 per second (ips) in carotid chemoreceptors (Band and Wolff, 1978) to over 1000 ips for Pacinian corpuscles (Martin, 1985). Since each such impulse involves some small but finite energy cost to the animal, the question arises as to what the benefits are at high rates of neuronal firing. Recordings from single nerve fibres are possible in the laboratory and the use of averaging techniques with a known, repetitive input can often be used to show how the unit is transmitting information. The most common method of information transmission appears to occur by varying the interval between each impulse, this encoding scheme is commonly called pulse frequency modulation (PFM). In animals, the recorded signals are often so variable that the averaging of many cycles is needed to extract the original input from the firing pattern of a single nerve. In the wild, an animal could not afford to wait for the signal to be repeated before reacting correctly, rather it must respond to its first occurrence. Few biological systems are actually dependent on single neurons, instead there is convergence of many equivalent sensors onto many parallel targets and so averaging is done by simultaneously combining the input of multiple afferents (spatial rather than temporal averaging) (Matthews, 1972).

1.2 Comparison of PFM and binary information transmission systems.

The transmission of information as impulses is widely used in modern communication systems and the encoding method of choice is normally a binary pulse code transmitted at a fixed rate over a single channel. This system has the advantage of high rates of transmission; much more information can be transmitted per unit time than with PFM but it is much more vulnerable to errors (Stein, 1967b). The introduction of error correction protocols involves redundancy and this can severely reduce these theoretical transmission rates. In addition the targets for much of this information are digital devices which are designed to deal with discrete digital information rather than continuous analog signals. Biological systems, by comparison, react to analog signals from the environment and produce an immediate graded response. The nature of a hostile world also requires a degree of redundancy and fault tolerance not yet found in electro-mechanical systems.

Bayly (1968) showed that the encoding of a signal using impulse frequency modulation (IPFM) produces a frequency spectrum consisting of a single component at the signal frequency (f_s), without any side bands, and a series of components at the carrier frequency (f_c) and its harmonics, each with a family of side bands ($\pm f_s$). The recovery of the signal from such a system can be achieved by a very simple low pass filter if the frequency components of the signal are much lower than the carrier frequency (see figure 1).

The resolution of this kind of system is limited by the modulation depth, the presence of noise components due to the carrier frequency and its associated harmonics and

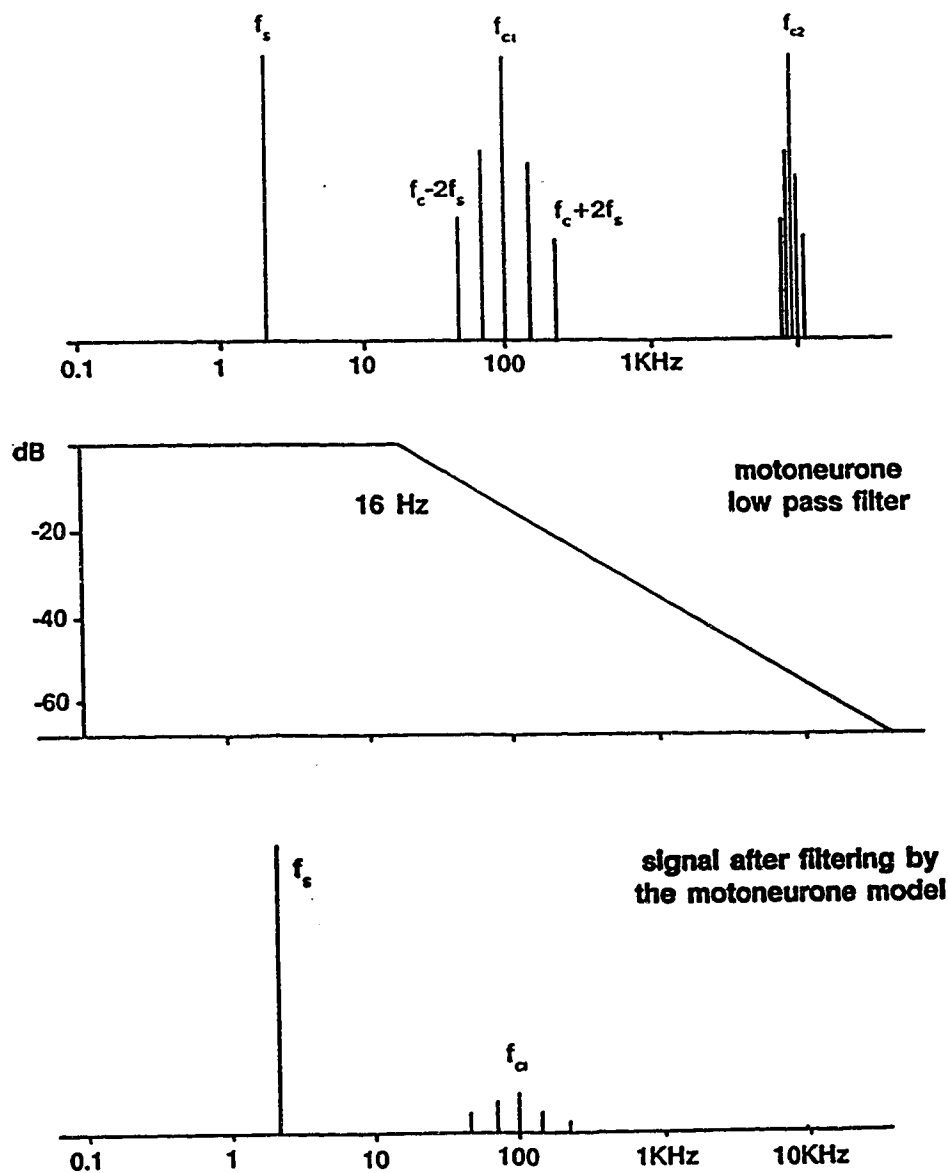


Figure 1 Recovery of information from a frequency code using a low pass filter.

Top: Fourier spectra for an IPFM coded 2 Hz signal (f_s), with a 100 Hz carrier rate (f_{c1}) or 10 KHz (f_{c2}). Note sidebands either side of carrier frequencies. Middle: Gain plot for a simple low pass filter with a 16 Hz cut off frequency. Bottom: Fourier spectra of A after passage through the filter B. Note the reduced size of carrier components at f_{c1} and total loss of those associated with the alternate carrier at f_{c2} .

distortions caused by the low pass filter recovery method. The size of the noise components due to the carrier frequency in the recovered signal is dependent on the separation between the carrier frequency and the filter cut off frequency. Thus, distortion can be reduced by increasing the separation between them, for example by increasing the carrier rate from 100 Hz to 10 KHz as in figure 1. Alternatively the filter cut off frequency can be reduced but this also limits the bandwidth of the signals that can be transmitted.

Bayly (1968) also showed that in addition to raising the effective carrier rate, the presence of several parallel carriers improves the signal to noise ratio (SNR: i.e. mean/(2 standard deviations)) by about the number of channels. When the channels are totally independent carriers with non-identical carrier rates the signal component will be common in all the channels and will be reinforced while the distortions due to the carrier rates will be dispersed and so not reinforce each other. If the carrier rates are identical but out of phase, the carrier components from the different channels will cancel each other out, while the signal component will be reinforced (Terzuolo, 1970).

From this we can see that increasing the firing rates or introducing more channels (nerve fibres with sensory endings) should result in more information available to the nervous system per unit time. Both of these methods would involve some cost. Having more channels would involve the production and maintenance of the extra nerve fibres and associated sensory endings, representing an added metabolic load. Increasing the firing rates would only involve the added cost of conducting and transmitting each action potential, and in most cases would also involve the participation of other neurons in setting gain parameters.

1.3 Limitations on the conduction of action potentials

What are the costs associated with action potentials? Each action potential is caused by a voltage sensitive local change in the membrane conductances of K^+ and Na^+ which causes a local change membrane potential which spreads by passive conduction along the axon. The action potential is actually driven by the maintained differences in ionic concentrations of K^+ and Na^+ across the fibre membrane which causes currents to flow in response to changes in ionic conductance. Though these ionic concentration gradients need energy to maintain them, each individual action potential causes only a very small degradation of this gradient and so most axons are capable of transmitting thousands of action potentials long after metabolism has been blocked (Brink et al., 1952).

In fact the limitations on discharge rates are governed by the properties of the excitable membrane and include:

- (1) The duration of each action potential.
- (2) The duration of the following absolute refractory period.
- (3) The input time constant.
- (4) The depth of after-hyperpolarization
- (5) Mechanisms of accommodation or adaptation.

(See Stein 1967c and Kuno and Miyahara 1968).

Based on these factors it was concluded that firing rates of up to 1000 ips are possible and these are indeed seen in dorso-spinocerebellar tract (DSCT) cells (Kuno and

Miyahara, 1968) though the most commonly seen upper limit is between 100 and 200 ips for most kinds of tonic receptors (Matthews, 1972).

Each action potential will degrade the differential ionic concentrations needed by the cell to enable it to conduct later action potentials and to maintain its internal functions. Restoration of these ionic concentrations has a metabolic cost, primarily through the breakdown of ATP by the Na^+/K^+ ionic pump. The recovery cost is estimated as $93\mu\text{cal/g}$ (Ritchie, 1974) for each single impulse based on heat, oxygen and optical methods, but this value is not a constant. It reduces with both increased duration and increased frequency of firing so using fewer neurons at higher rates would appear to be more efficient. The mean firing rate must be sustainable, the energy consumption is in the form of ATP used by the Na^+/K^+ pump and this has to be regenerated by the cell. If this could not be produced fast enough it could limit the maximum firing rate. Connelly (1959) showed that the oxygen uptake of excised frog sciatic nerve, starting from $1.5\mu\text{M O}_2/\text{g.hr}$ increased when the nerve was tetanised and that this increase reached a maximum of $1\mu\text{M O}_2/\text{g.hr}$ (total $2.5\mu\text{M O}_2/\text{g.hr}$) at a tetanising frequency of 100 Hz. The kinetics of heat production followed a similar course. This indicates that the maximum metabolic rates within the nerve fibre should only be able to sustain continuous firing rates of less than 100 Hz. However this rate is based on the metabolism of a whole nerve and does not take into account its heterogeneous composition. With C fibres at 20°C Greengard and Straub (1959) showed that depletion of ATP was possible at rates as low as 50 Hz but at the more physiological rate for these small fibres of 15 Hz, depletion of ATP and the build up of breakdown products did not occur. Since the numbers of ions lost with each action potential are small when compared to the total number of ions found within each axon many fibres can

Cost of conducting action potentials

Frog sciatic nerve $T = 20^{\circ} \text{C}$

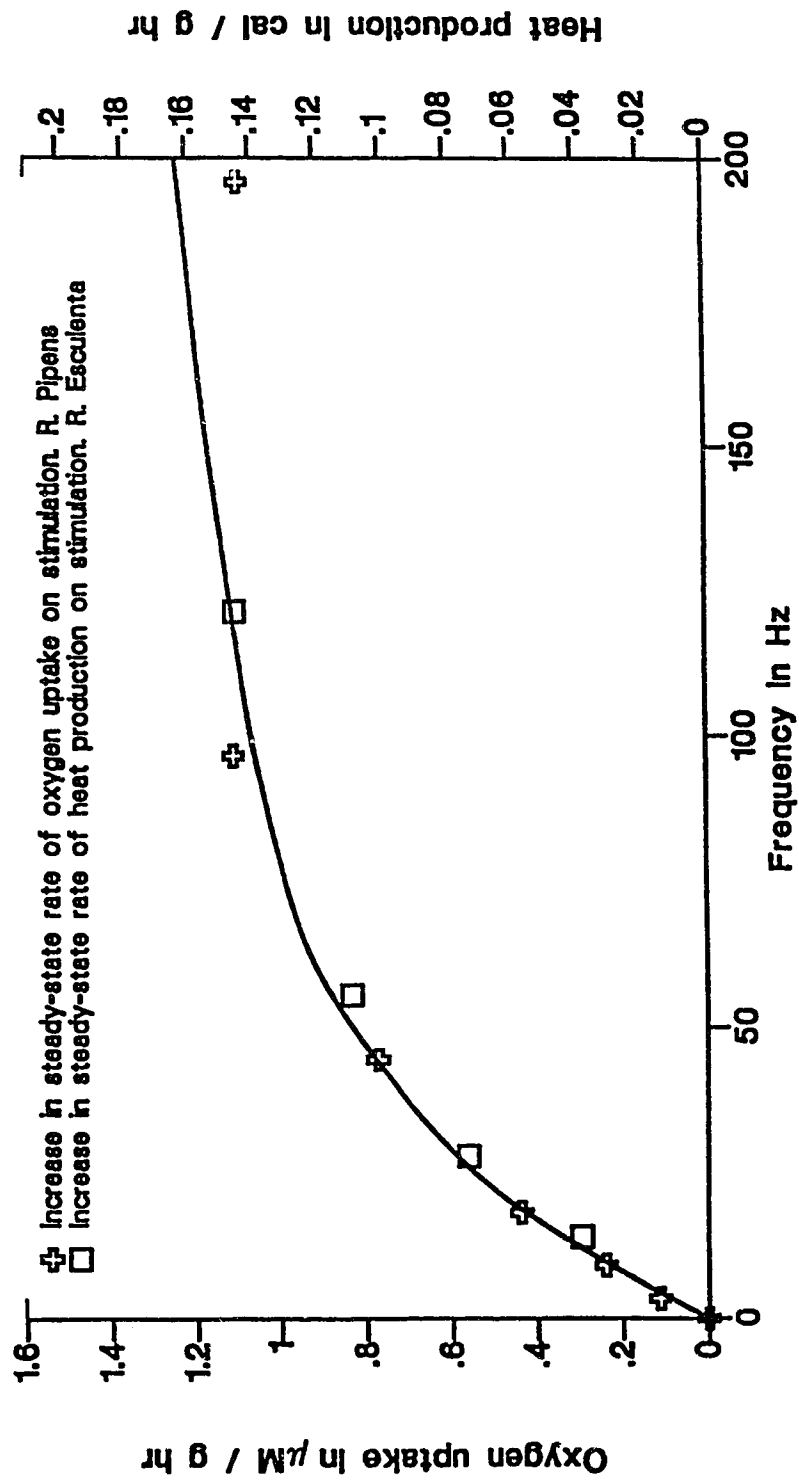


Figure 2 Energy consumption of a conducting nerve as a function of stimulation frequency. Crosses O_2 consumption in $\mu\text{M/g hr}$ (left axis). Squares heat production in cal/g hr. (Replotted from Brink, Bronk, Carlson, and Connelly 1952).

actually conduct impulses at rates higher than these sustainable ones for quite long periods. Eventually the membrane potential starts to run down and conduction is blocked unless the fibres have an opportunity to repay the accumulated large oxygen debt. The additional oxygen uptake following conduction of action potentials can be blocked by 0.1 milli-molar azide. When so blocked, it has been shown that α -fibres can conduct up to 2 million action potentials before failure sets in (Brink et al, 1952). This would indicate that even if the long-term sustainable firing rates are as low as 50 to 100 Hz, the fibres have the ability to maintain higher firing rates for quite significant periods.

1.4 Costs of synaptic transmission.

As we have just seen, the cost of conducting large numbers of action potentials is quite low. However when the action potentials reach the end of a nerve fibre they have to be passed onto the next neuron in one form or another. In most mammalian neurons this is achieved by a chemical synapse. The current model of synaptic transmission, based on the neuromuscular junction, involves at least 9 steps;

- 1 The arrival of the action potential in the pre-synaptic terminal causes the opening of Ca^{2+} channels and the possible additional release of Ca^{2+} from internal stores.
- 2 The increase in internal $[\text{Ca}^{2+}]$ causes the fusion of vesicles with specialisations of the pre-synaptic membrane.
- 3 After the vesicles fuse to the plasma membrane their contents (transmitter) are released into the synaptic cleft.

- 4 The transmitter then diffuses across the cleft and, by interacting with specific receptors on the post-synaptic membrane, causes specific changes in ionic conductance.
- 5 The transmitter must then be removed from the synaptic cleft. This can be done by breaking it down into inactive precursors, by active uptake by the surrounding cells, and/or passive diffusion.
- 6 The vesicle membrane has to be recovered from the plasma membrane or resynthesized.
- 7 Internal $[Ca^{2+}]_i$ must be restored to normal.
- 8 Transmitter lost to other cells or destroyed must be resynthesized.
- 9 The vesicles must then be refilled with transmitter.

Although some alternative models do not rely on vesicles actually fusing with the plasma membrane (step 2), they require the Ca^{2+} mediated movement of transmitter from the vesicle through the cytoplasm into the synaptic cleft. With the above model in mind we can see that energy is possibly needed for steps 2, 5 (uptake), 6, 7, 8 and 9 and that steps 2, 5, 7, and 9 may be rate limiting.

The neuromuscular junction is an example of a very large synapse which is quite specialised, but its size and peripheral location make it ideal for general study. Continuous stimulation at 2 Hz causes the size of end plate potentials (EPPs) recorded from muscle fibres to fall. This reaches a plateau under normal conditions, but inhibition of acetylcholine (ACh) synthesis will cause the EPP to fall to 0 (Ceccarelli and Hurlbut, 1975). The plateau therefore represents the level at which synthesis of new transmitter balances the

expenditure with each action potential. This rate of replenishment (≈ 3000 quanta per min: Capek et al, 1971) can be sustained for a variable time and then fails for unknown reasons (Van der Kloot, 1977). ACh synthesis can be blocked by Hemi-cholinium no.3 (HC-3) but is unaffected by the addition of choline chloride to the bathing media (Capek et al, 1971). Ceccarelli et al (1973) in combining electron-microscopic techniques with electrophysiological ones was able to show that for the frog neuromuscular junction both transmitter (ACh) and vesicle numbers could be depleted. With continuous stimulation at 10 Hz depletion of both vesicles and ACh occurred in about 15 minutes. Continuous stimulation at 2 Hz for 3 hours depleted ACh without depleting the amount of vesicles while intermittent stimulation (2 Hz for 2 hours with $\frac{1}{2}$ hour rests) produced a depletion of transmitter and vesicles after 6-9 hours. From this they concluded that transmitter could be resynthesized at about 140 quanta/sec and that vesicles can be reformed at at least this rate for up to 4 hours. This involves recycling membrane equivalent to about 5 times the surface of a typical terminal. In all of these experiments the terminals eventually lost their ability to synthesize transmitter before they ran out of vesicles. Since the terminals were separated from the cell body this loss of function could be due to the absence of synthetic activities normally provided by the cell body.

Wiley et al (1987) recently showed similar effects of stimulation on vesicle numbers in the mammalian superior cervical sympathetic ganglion in vivo. Stimulation at 10 Hz produced a rapid reduction in vesicle numbers to a stable, frequency-dependent level with some associated expansion of membrane area. Recovery of the excess membrane took place over a period of up to 1 hour after the 20 minutes of stimulation at 20 Hz. Thirty minutes of stimulation at 40 Hz produced membrane changes that did not fully recover indicating

possible pathological injury. The upper limit for prolonged and sustained firing was about 20 ips, much less than the sustainable firing rate of the axons. It should be also stated that these rates are far higher than the physiological ones, typically cervical sympathetic ganglia cells only fire at 1 or 2 ips with bursts reaching 30 ips (Skok, 1973). This fits with the calculated values of 15.4 (McCandless et al, 1971) and 18.6 ips (Birks and MacIntosh, 1961) as the maximum rates these cells could be expected to fire indefinitely. For the cat monosynaptic reflex pathway, transmitter production appears to balance expenditure at rates of 40-50 ips (Esplin and Zablocka-Esplin, 1971). Interestingly 54 ips is the mean firing rate of triceps surae Ia afferents during normal walking in the cat (Prochazka et al, 1989).

The common factor in all these experiments is the assumption that the amount of transmitter released is a fraction of the available pool (a first order depletion process) but once activated, transmitter replenishment occurs at a constant rate (zero order replenishment). Experiments with HC-3 and choline chloride (Capek et al, 1971, McCandless et al, 1971, Skok, 1973) all support these assumptions for periods of up to 2 hours after which synthesis starts to fail. Changes in the rate of synthesis were seen in the spinal monosynaptic pathway after stimulation at 500 Hz for 3 hours (Zablocka-Esplin and Esplin, 1971) indicating that the synapses can adapt to higher firing rates if exposed to them for long enough. Such changes were not lost after 16 hours; these long term changes are thus not likely to be caused by local regulation of transmitter production but instead could be indicative of enzyme induction (production of additional enzymes for transmitter synthesis). This could indicate that support of higher firing rates would require the production of more enzymes and other materials to support higher consumption of transmitter.

The dependence of synaptic transmission on the available energy supply was studied by Yamamoto and Kurokawa (1970) who showed that for olfactory cortex slices maintained in vitro, reductions in ATP level of 20% diminished the post-synaptic potential by 93%. Any further reduction of ATP concentration totally blocked transmission. Measurement of oxygen consumption as a function of frequency in sympathetic ganglia by Larrabee (1958) showed a 42% increase at 15 Hz. Above 15 Hz there was no further increase, indeed the amount of oxygen consumed per impulse declined as the frequency increased. From this Larrabee concluded that "a fundamental property of neuronal metabolism is a decrease in the amount of oxygen consumed per individual nerve impulse as the frequency of action potentials is increased and as the interval allowed for recovery between successive impulses is thereby decreased." That the O₂ consumed per impulse at even these low frequencies reduces with frequency indicates that full recovery is not made between each impulse but that some debt has to be carried forward. By varying the O₂ concentration Larrabee also showed that the diffusion of oxygen into the ganglion was not the limiting factor in controlling synaptic transmission rates. The mechanism of synaptic transmission does appear to be the limiting factor in controlling impulse rates, the costs of bursts of higher than normal firing rates producing a debt that has to be recovered afterwards and so limits the length of high frequency bursts.

From this it appears that the cost of transmitting information in the nervous system is mainly due to the costs associated with chemical transmission at the synapse and that this step, while providing a large amount of flexibility for information processing, is normally the rate-limiting one.

1.5 Measures of information and estimations of resolution

In order to evaluate information flow we need a way to measure the quantity of information reaching the central nervous system. Information can be defined as the degree of order in the system which is the negative of the entropy (uncertainty). The most common measure of information capacity is bits per second. This is the logarithm to the base 2 of the number of discriminable categories in one second (Ash, 1965, Stein, 1967b).

According to Shannon and Weaver (1949) the information content of one channel can be described by the relation:

$$H(A) = -P(A)\log_2 P(A)$$

Where $P(A)$ = Probability of event A.

and for two perfectly independent channels

$$H(A,B) = H(A) + H(B)$$

but if the channels have any degree of redundancy then

$$H(A,B) < H(A) + H(B)$$

In simple terms this means that if redundancy exists, the information carried by the two channels is less than the sum of the information carried in each individual channel. The gain in information in decoding the same information twice (perfect correlation) was shown by Stein (1967b). Thus the gain in information content from multiple channels is reduced by any correlation between channels.

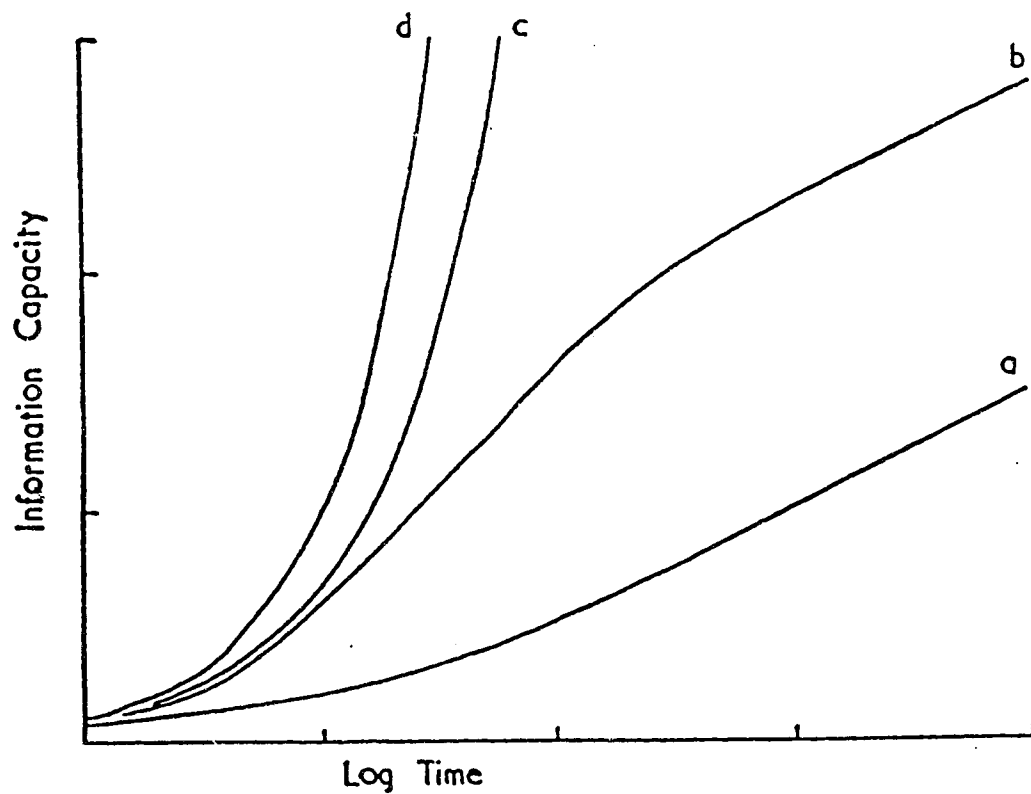


Figure 3 Schematic representation of information capacity as a function of stimulus duration for a neuron, a) Discharging randomly and using a frequency code, b) Discharging fairly regularly and using a frequency code, c) using a binary pulse code, and d) using an interval code. Reproduced with permission from Stein 1967b.

In physiological terms bits per second is a unsatisfactory measure as biological systems are transmitting information about continuous analog processes. Since we will be estimating the instantaneous resolution (number of discriminable levels), we have used the signal to noise ratio (SNR) and not converted this into bits. Using information theory and some early data, Stein (1967a,1967b) proceeded to look at the theoretical information capacity of neurones using different coding properties and different noise models against time. Stein and Matthews (1965) estimated that a single Ia muscle afferent could transmit 64 levels (6 bits of information) in one second and the presence of fusimotor activity would reduce this to only 16 levels (4 bits) because of the associated increase in inter-spike variability and despite increasing the firing rate of the afferent. In looking at multiple cells Stein (1967b) also proposed that the maximum information of multiple cells increased by $0.5 \log_2(N)$ per unit of time. From this and later work (Stein and French, 1970) it was possible to show that noise in the form of interspike variability could be beneficial and in fact could increase the linear range and dramatically reduce distortions due to phase locking. Against this, variability also caused a reduced sensitivity at all frequencies and a loss of frequency response at high frequencies. An example of a neuronal system in which such effects are seen in real life and which has been studied in detail, is the fusimotor control of proprioceptive feedback in mammals.

Inbar et al (1979) and Rudomín (1980) studied the correlations between spike trains from pairs of muscle spindle afferents. During ramp stretch, with intact ventral roots (fusimotor action present) no correlation was seen but when the ventral roots were cut (to stop fusimotor action) a small amount of correlation was seen. This correlation had a 60 Hz period and was thought to be due to very small amplitude vibration induced in the

puller by line noise. Therefore the gamma system appears to decorrelate the activity of different muscle spindles responding to a common input. In the case of ensembles, the gamma system would therefore be expected to increase the information transfer because it would both increase the mean rate and reduce interchannel redundancy (cross correlation). This is not inconsistent with the conclusions of Matthews and Stein (1969) for single muscle spindles, namely that the fusimotor system, by introducing interspike variability, would limit information transfer rather than enhancing it.

1.6 Algebraic summation in motoneurons

In order to use the information carried by multiple channels the signals must be brought together in a single place. In the nervous system this is done by integration of the afferent input by a second order neuron. In the monosynaptic reflex this cell is the motoneuron. The incoming all-or-nothing pulses are converted into ionic currents at each synapse independently. These currents then flow into the soma where they combine to produce a net depolarization which drives the spike producing mechanism of the axon hillock or first segment.

For the motoneuron it has been shown that the net synaptic inputs sum algebraically across the whole of the "primary range" (representing 85% of the resulting force output) (Granit *et al*, 1966a). In the secondary range, where the frequency force response of the muscle fibres is rapidly falling off (Kernell, 1983) the slope of the frequency-current (f-I) relationship greatly increases and the synaptic efficacy of both EPSPs and IPSPs (excitatory and inhibitory post synaptic potentials) is reduced due to the inactivation of Na^+ channels

by blocking caused by the experimental current source (Granit et al, 1966b). True synaptic inputs are better able to induce higher firing rates without causing inactivation as the input is more evenly dispersed across the dendritic membrane, rather than concentrated round the electrode in the soma. This produces a greater net current without causing the very large local charge densities that inactivate the Na⁺ channels.

By comparison DSCT neurones, which also receive monosynaptic input from muscle afferents, produce much higher firing rates (800-1000 ips) and can fire in response to a single large EPSP. Unlike the spinal motoneurons, the frequency current relationship is not a straight line as the frequency tends towards a limit imposed by the membrane time constant and the absolute refractory period (Kuno and Miyahara, 1968). As with motoneurons, the size of EPSPs is relatively unaffected by postsynaptic hyperpolarization and this, coupled with the regeneration of EPSPs after an action potential (Curtis et al, 1958, Eccles et al, 1961), would support the idea that the EPSPs originate from a site not invaded by the action potential and is more likely to be on the dendrites as opposed to the soma of the cell.

1.7 Summary of aims of experiments.

The large collection of Ia muscle afferents recordings was kindly made available to me by Dr. M. Hulliger of the University of Calgary. These afferent were recorded with and without fusimotor activity in response to a standardised ramp-and-hold signal as an identification test. This has provided a large data base with which to investigate, for real populations of afferents, what factors affect the resolution of information transmitted in the

nervous system. With the wide diversity of encoding possibilities it was decided that it would be reasonable to just consider the resulting membrane potentials of an idealised second order cell (in this case based on the motoneuron).

In order to investigate these effects representative populations were constructed from the available data base and combined using a simple motoneuron model. The resulting output could then be analyzed to give realistic SNR values.

2 METHODS

2.1 Acute recordings

The data for this study were recorded from over 100 cats in Dr. M. Hulliger's laboratory at the Brain Research Institute in Zurich. These experiments were motivated by chronic recordings previously done by Dr. A. Prochazka, Dr. P. Trend and myself and I was able to visit Zurich to assist in the initial processing and collection of this data from several of these experiments.

2.1.1 Preparation.

Adult cats weighing 2-3.5 Kg were anaesthetized with pentobarbitone (40 mg/Kg i.p.) and additional doses were given i.v. to maintain a surgical level of anaesthesia. The cats were intubated to permit artificial respiration if necessary and to maintain a clear airway.

The right hindlimb was extensively denervated, sparing only the soleus muscle. The spinal cord was then exposed by a laminectomy from L1 to S2 and the dorsal and ventral roots were sectioned to prepare for splitting.

The cat was then mounted in a rigid frame and the soleus muscle attached, via a semiconductor proving ring force gauge, to an electromagnetic servo controlled muscle puller (Ling Dynamics). Sinusoidal and ramp-and-hold stretches with peak to peak amplitudes of 8 mm and peak plateau durations of 30-120 sec were used to bring the muscle to a length corresponding to 2 mm below the physiological maximum (in short -2 mm). The level of mechanical noise in the stretcher was kept below 0.1 and 0.5 μ m for frequencies below and above 10 Hz. To this end heavily low-pass filtered input signals (ramps) were used.

2.1.2 Selection of neurons

Primary afferents were then isolated in the dorsal root filaments and identified on the bases of conduction velocity (≥ 70 m/sec) and dynamic sensitivity in response to stretch of 8 mm at 10 mm/sec. Fusimotor fibres were then selected by electrical stimulation of ventral root filaments. A force gauge attached to the muscle was used to detect any unwanted α activity, the filaments then being split until the α -activity was lost. The fusimotor type was then identified by the change in response of the primary afferents to ramp stretch in the presence and absence of fusimotor stimulation and classed into the six categories of Emonet Dénand et al (1977). Only those fusimotor (γ) motoneurons falling into categories I and VI have been used in this study.

2.1.3 Recording of data

The Data was recorded on a PDP 12 minicomputer using custom written software which stored the interspike intervals to a $10\mu\text{s}$ resolution. The data format was chosen for speed of writing to ensure no spikes would be missed rather than later ease of use. It was therefore necessary to write a translation program (Extract) to recover the data.

2.2 Synthetic firing profiles

Due to the initial difficulties in transferring the complete banks of data from Dr. M. Hulliger's LSI/PDP computer systems (initially in Zurich and later in Calgary) to the Olivetti M28 (IBM AT compatible) computers at the University of Alberta the initial studies were done using synthesized firing rate profiles. These were based on Dr. M. Hulliger's response plots of spindles to a standard 8 mm ramp-and-hold. On the basis of these plots the firing rate of each unit was determined at 6 points through the imposed ramp stretch and cumulative population curves were produced. These were then used to estimate the firing frequencies needed to produce synthetic populations of 3, 6, 12, 25 and 50 units with appropriate distributions. This was done by dividing the cumulative probability curves (Figure 9) horizontally by the desired population size plus 1. Where these lines crossed the target population curve then indicated the appropriate frequencies needed for the desired sub-population.

Outputs from a voltage divider and a white noise generator were then fed into a voltage controlled oscillator (VCO) and the output sampled on a CED 1401 (Cambridge

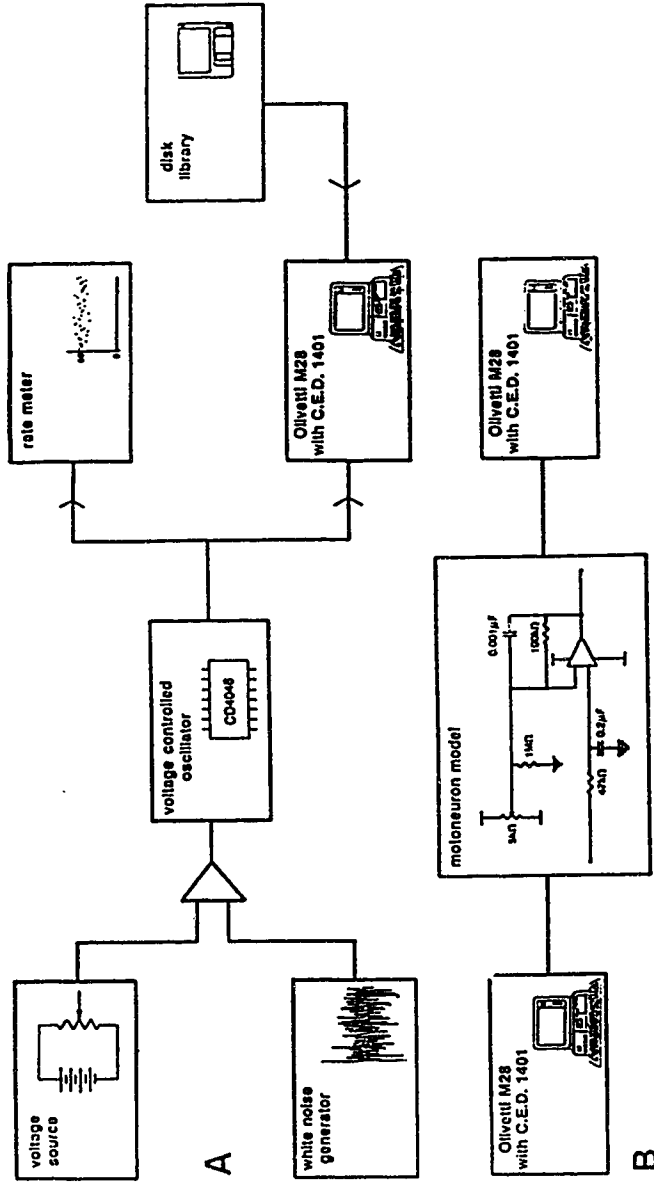


Figure 4 Schematic representation of the experimental setup.

A) Generation of model unit spike trains.

To generate the model unit spike trains the Voltage source was set to give the required output frequency (measured with the rate meter) and then noise was added to produce interspike variability. The resulting output was then digitised by the computer system. This stage was later replaced by a library of muscle spindle recordings on disk.

B) Conversion of pdfs into a model motoneuron membrane response.

The pdf functions generated in A were played out at 1 kHz through the simple motoneuron model (centre) and sampled at 2 kHz by the second computer system.

Electronic Design) laboratory interface attached to an Olivetti M28 microcomputer (figure 4A), so that any combination of firing rate and contaminating noise level could be mimicked. Each unit was modeled by selecting the base frequency needed from the cumulative distribution chart (figure 9) and by monitoring the digital rate meter, the VCO was set to produce that frequency. Interspike variability was then added by setting the white noise generator to the desired level (0 to 10) and the resulting output sampled by the computer. The population distributions for passive, fusimotor dynamic stimulated (γ_d) and fusimotor static stimulated (γ_s) populations were then used to select the synthetic units which were then combined to produce the probability density functions (pdf) for populations of 3, 6, 12, 25 and 50 units. Populations with different added noise levels (manifested as variability in interspike interval), ranging from a theoretical pure signal (noise generator output level 0), through levels appropriate for γ_d (4) and γ_s (6) stimulation to an excessively noisy signal (10) were also constructed. For example the population 3 'pure' pdf was made using sampled sections with the voltage input to the VCO set to give spikes at 55, 80 (inset on the left of figure 11) and 115 ips. Each pdf then represented the net input to the target motoneuron from each population size and with different amounts of interspike variability (noise). A bin width of 1 ms was chosen to simplify the modelling of the motoneuron (see 2.4). These pdfs were then passed through the simple motoneuron model and the resulting "membrane potential" was measured for each of the populations (figure 11). This was fitted to a straight line and the root mean square about this line was calculated as a measure of the residual noise.

2.3 Real unit firing profiles

2.3.1 Population distributions

Due to limitations in the resolution of the working plots used as the initial bases for the above work the original data for 212 spindles, with and without γ stimulation, recorded in response to standardised ramp-and-hold stretch during the identification phase of acute reconstruction experiments, (as described in 2.1.2) were obtained on disk from Dr. M. Mulliger. The Extract program was then used to print out, for each unit, the firing frequencies at intervals throughout the ramp-and-hold cycle. The frequency at each point was taken as the mean of the three closest intervals to insure that the value used was representative of the actual unit firing rate and not an isolated spike due to noise or false triggers in the recording equipment. Unfortunately, with the very low firing frequencies of the passive units this sometimes meant that the intervals used for the first and second points overlapped and any dynamic acceleration component would be reduced. By the third point the firing frequencies were high enough to ensure that the windows did not overlap. Each peak frequency was based on an average of 5 spikes centred on the shortest interval since a more accurate value was wanted for the calculations of dynamic index (DI) and the higher rates enabled more points to be considered within a small time window. These values were then used to confirm the population distribution analysis (figures 6, 7, 8 and 9) and then combined into typical population responses (figure 10).

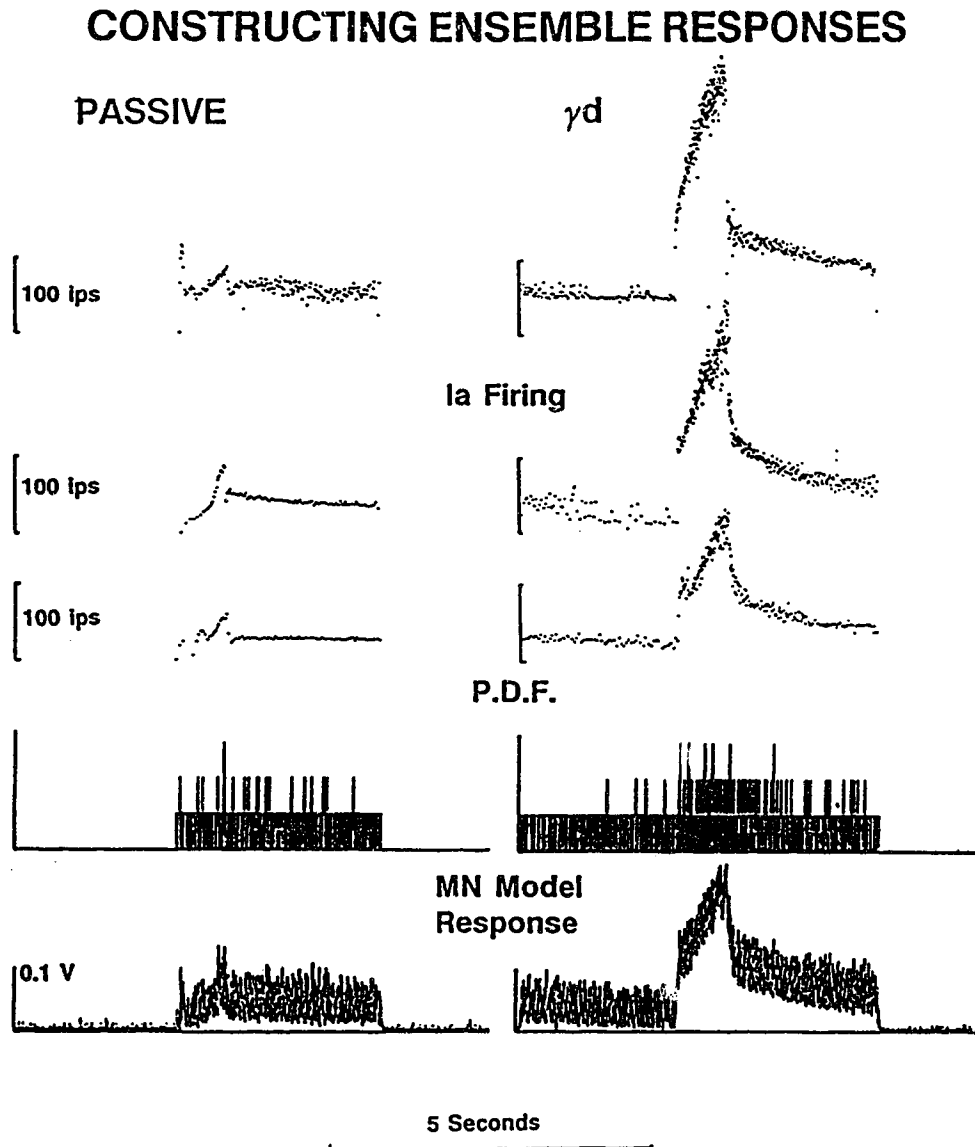


Figure 5 Construction of ensemble responses.

The individual responses of the three typical Ia afferents (top) with and without γ stimulation, were combined to produce the probability density functions (P.D.F.s) shown. These P.D.F.s were then passed through the motoneuron model to produce the model response (bottom).

2.3.2 Combination into populations

Since the data were recorded in a file format appropriate to the PDP computer system a simple Pascal program (Extract) was written to extract and display each response on screen with the values of mid-slope firing rate, peak firing rate and dynamic index. These values were then used to make up distribution histograms for the real populations and then used to select the units to be used for each population (passive, γ_d and γ_s in each of 3, 6, 12, 25 and 50 units). Since the original units were recorded from actual spindle afferents no additional noise was added as the units recorded would have at least the physiologically appropriate amount already.

The Extract program was then used to build bin histograms (1 ms bin width) of the selected populations which were then stored in the correct format for loading into the CED 1401 MassAvg program. These populations could then be passed through the motoneuron model. This process is illustrated in figure 5. In this figure the three units shown (top) are combined to produce the pdf which is then passed through the motoneuron model to produce the modeled response at the bottom. Notice how even with the γ_d stimulated units the 1 ms bin width pdf produces an apparently poor representation of the neuronal activity as the net firing frequency is too low to fill most of the bins. For this reason 10 ms bin width histograms have been used for illustrative purposes in figure 10.

2.4 Construction of the motoneuron model

Based on the studies of Kirkwood and Sears (1982), Burke (1967) and Redman and Walmsley (1981) a typical motoneuron EPSP was identified to have a 10 to 90% rise time of 0.8-1 ms and a mean half width of about 4.7 ms. With the bin width of the population histograms chosen to limit the pulse width to 1 ms (and so limit the rise time) a fairly simple RC circuit could be used to shape each pulse to the desired single EPSP shape. This circuit is shown in figure 4b.

For this model to be useful it has been necessary to assume that each EPSP adds algebraically. This means that every afferent synapses must be sufficiently spatially distinct to prevent the local changes in membrane potential at one synapse changing (and for an EPSP reducing) the driving potential at a second synapse. Since synaptic contacts are situated mostly on the dendrites, only 4% being on the soma, (Jack et al., 1970) and many unitary EPSPs are generated at multiple sites (Jack et al., 1970) it is felt that this is a justified assumption. If each event is independent and injects a fixed amount of current into the target cell and if two events occur at the same time the soma should only see a single event of double size. The algebraic summation of EPSPs has been shown by Burke (1967) and the agreement between summed unitary and net compound EPSPs has been shown by Prochazka (1989a). The equivalence of injected and synaptic currents in motoneurons has also been investigated (Schwindt and Calvin, 1973), while supraspinal stimulation can sometimes change the f-I curve of motoneurons in most cases the two types of current summed algebraically to produce a change in firing rate. On this basis it was decided that a probability density function with the appropriately small bin width was an adequate

representation of the synaptic barrage from multiple independent afferents, two independent events occurring at once being represented as a single double size event. With high mean firing rates (in excess of 300 ips), EPSP summation in ensembles does become non-linear (Winchester, 1988), but this is beyond the range of mean rates occurring with the standard displacement signal used in this study.

2.4.1 Passage through the motoneuron model.

The 15 resulting probability density functions were then played out of a CED 1401 interface into the simple motoneuron model at 1 KHz and the response sampled into a second 1401 at 2 KHz. The responses of the model to the population ramp-and-hold were then exported into individual DOS text files for import into more general purpose mathematical programs.

2.5 Quantitative analysis.

Each modelled motoneuron response was then imported into individual SuperCalc 5 (or Lotus 123) spreadsheets so that a series of different calculations could be performed on each one.

First, each value was divided by the population size. This was to normalize the effect of each population on the theoretical target neuron so that each population represented the same total maximum depolarization. This is justified since the sub-populations were supposed to represent the same total input to the second order cell. As

the mean EPSP size decreases with increased connectivity (as a % of the available afferents population), the overall average EPSP amplitude, where non-connections = 0 are included, is estimated to be about $67\mu V$ for different size motoneuron populations (Kirkwood and Sears, 1982 and Prochazka, 1989a). Unit EPSP size does appear to be independent of the population size so potency is determined by numbers of units not their connectivity. (Kirkwood and Sears, 1976).

Next the instantaneous mean was calculated for each point (± 80 points) in the response. This was then used to calculate the standard deviation and coefficient of variance at each point. Due to the dynamic responses this method was not reliable at the turning points of the ramp-and-hold signal and so these regions were masked out and the remaining areas used to produce plots of coefficient of variance against mean input frequency for each sub-population, see figure 15.

2.6 Programming

Programs were written in Turbo PASCAL 3.0™ (MassAvg) and 4.0 (Extract) on a Olivetti M28™ (IBM AT compatible) computer.

Briefly these programs served the following functions.

2.6.1 MassAvg

This program is used to control the CED 1401 laboratory interfaces used in this laboratory and is a much larger general purpose program for experimental use. It is based on a kernel written by CED for Dr. A. Prochazka and myself to which I have added all the averaging functions, support for continuous replaying of data, special support for an event channel with instantaneous rate display, data export facilities and improved the use of the screen and keyboard. The use of the MetaWindow™ library of screen functions enables the program to run on a wide range of the video cards found on IBM compatible computers.

This program supports the sampling and display of up to 8 channels of analog data or two analog and one event channel at rates between 10 Hz and 67 KHz (faster with newer 1401 systems). The data sampled may be stored on disk for later retrieval or averaged using manually set markers. The averaging mode superimposes each selected sweep one at a time, allowing the user to adjust the alignment or deselect the sweep. The program first shows the average superimposed on the built up display of individual sweeps so that the scatter of the population can be seen and then displays the average on its own. The averages can then be filed. Reloaded averages can be treated as normal data if desired (enabling different averages to be superimposed or grand averages to be produced. Up to four channels of data at a time may be played out of the digital to analog converters (DAC) to drive other laboratory equipment such as muscle pullers, chart recorders or electrical circuits.

Hard copy can be produced on Epson compatible printers or on HPGL (Hewlett Packard Graphics Language) compatible plotters. Image transfer to paint programs (.PCX format) and vector graphics (HPGL files) is supported while raw data can be exported as ASCII text for use in other programs.

(The lab instruction book for this program is included as appendix A)

2.6.2 Extract

Since the raw data was stored in 7 large files with a special compressed format it was necessary to write a program to decode it. In order to support the Intel 6 byte real number format used by Turbo Pascal 3 and the IEEE standard 8 byte real, long Integer and Short integer numeric types used in the data files from the PDP/LSI environment it was necessary to use Turbo Pascal 4.0. This program performs the following functions.

- a) Decode and separate the data from bulk files written on the PDP computers.
- b) Display the data for each unit complete with the resting, half slope, peak and 0.5 s post peak (to calculate dynamic index) firing rates and print each display.
- c) Output to a file estimates of each units firing rate at identified points in the ramp-and-hold cycle.
- d) Build up the bin histograms from the selected units that could then be imported into the MassAvg program, from which they could be used to drive the motoneuron model.

3 RESULTS

3.1 Population distributions

Before any modelling of ensemble responses could be done it was necessary to know how the range of firing frequencies seen in the population changed with stretch and fusimotor drive. Using the individual printed plots produced by Dr. M. Hulliger and Dr. A. Prochazka of the responses of a large number of muscle spindle afferents it was possible to build up some idea of the behaviour and diversity of primary spindle afferent units to the standard ramp stretch. Since in the first few months of this study the frequencies had to be estimated from the printouts the accuracy was limited and mean frequencies had to be estimated by eye. In addition the limitations of the original plotting device had necessitated the averaging of frequencies above 125 Hz. This meant that the short interspike intervals associated with the highest firing rates were averaged with an adjacent interval and so the highest frequencies were always under-represented in the distributions. The general form of these distribution studies is shown in figure 6 where the distribution histograms of the three populations are shown for the three points in the stretch indicated on the left.

The passive group (no γ action) started with a very low mean frequency which increased with stretch. The addition of fusimotor drive increased both the initial frequency and the sensitivity to stretch. In addition the range of frequencies increased, especially for γ_d stimulation where there was a more skewed distribution of firing rates.

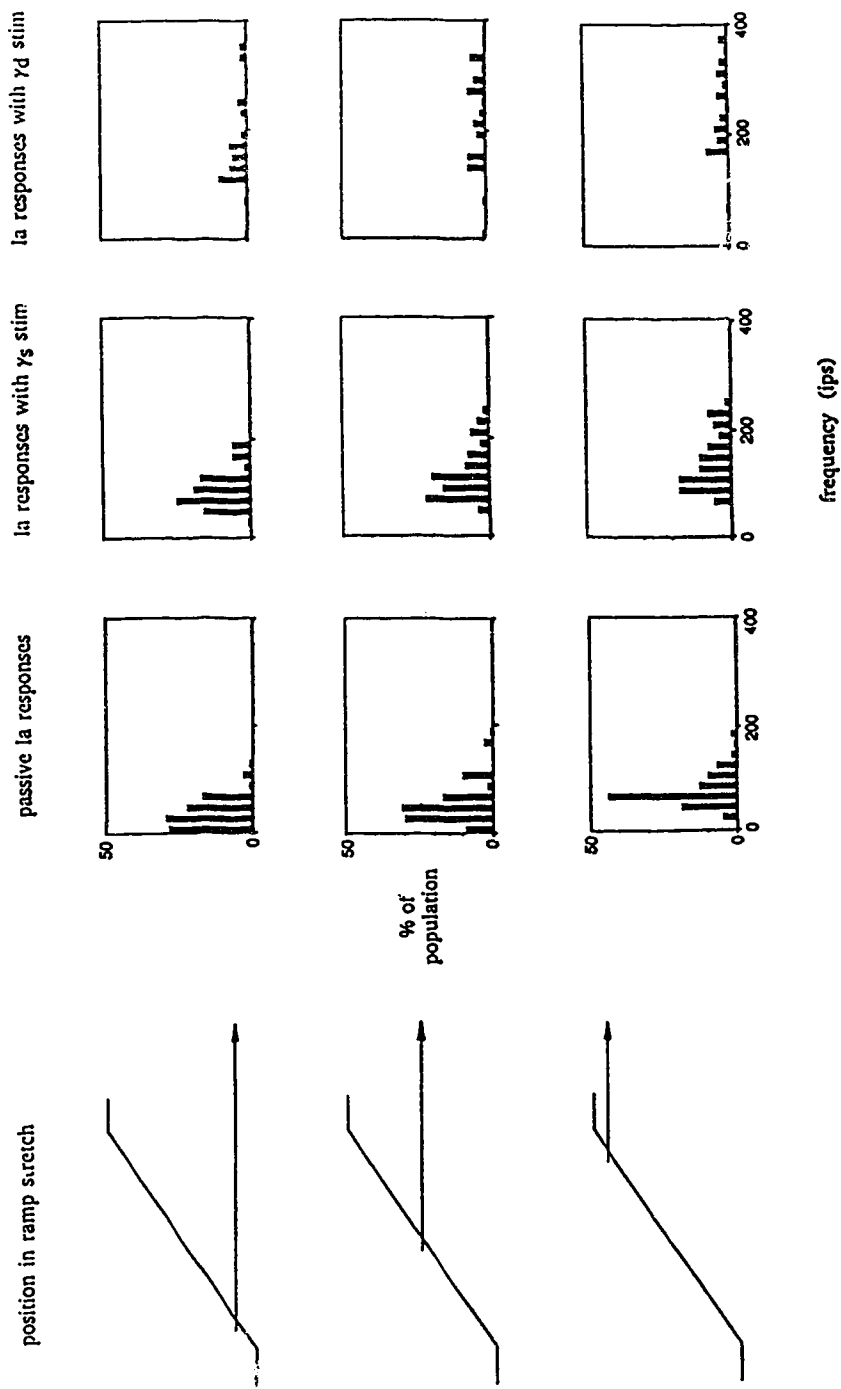


Figure 6 The frequency distributions of Ia afferent populations at three positions in a ramp stretch. Distribution of Ia afferent firing frequencies seen in cat muscle spindles during a ramp stretch. For each position in the stretch shown on the left the firing rate was measured for each unit under passive stretch and with fusimotor (γ_d or γ_s) stimulation (100 ips). The units were then grouped in multiples of 20 ips, y axis percentage of the population.

Frequency of Ia afferent populations during a ramp stretch ± 1 SD.
 Passive and with γ_s or γ_d fusimotor stimulation at 100 ips.

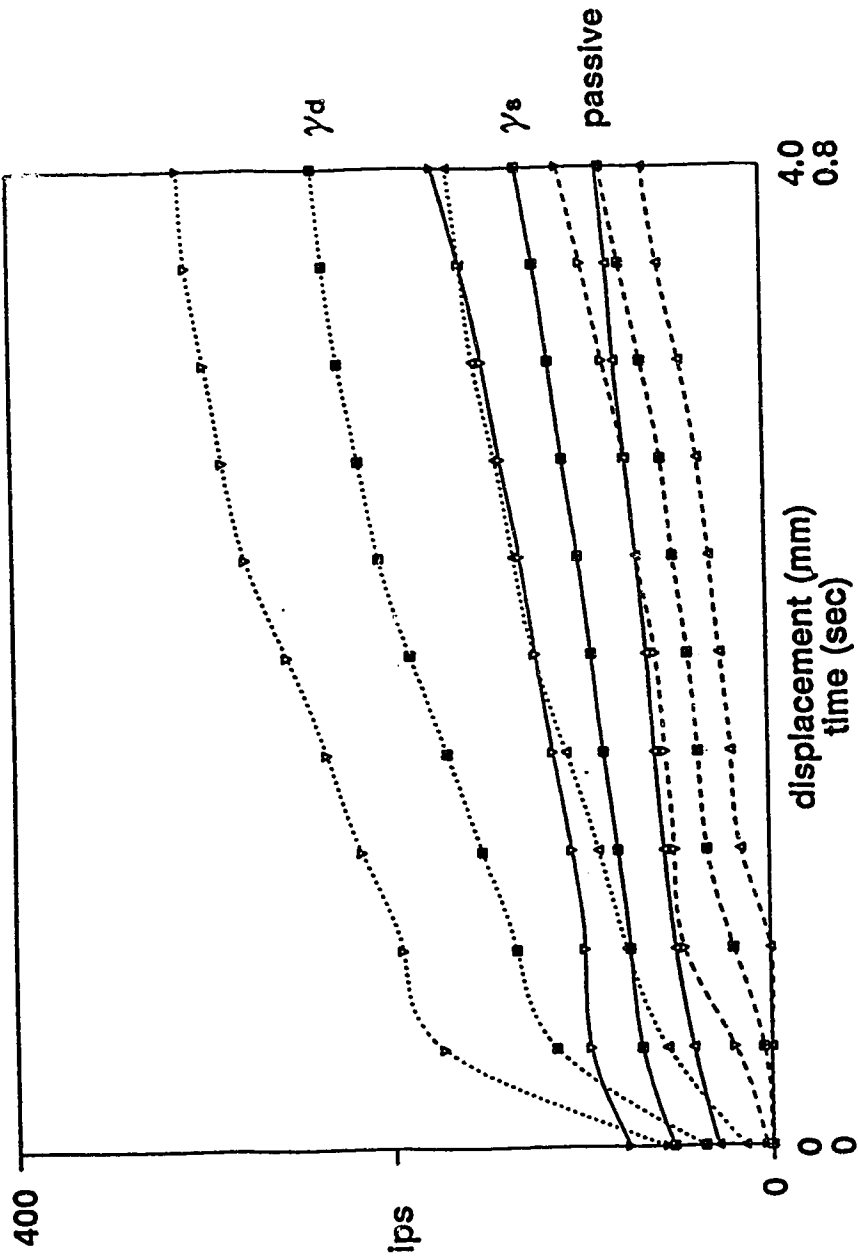


Figure 7 Frequency of firing in Ia afferent populations during a ramp stretch. The mean firing rate, with ± 1 standard deviation bands, is shown for populations of passive (dashed), γ_s stimulated (solid) and γ_d stimulated (dotted) primary muscle spindle afferents undergoing a ramp stretch.

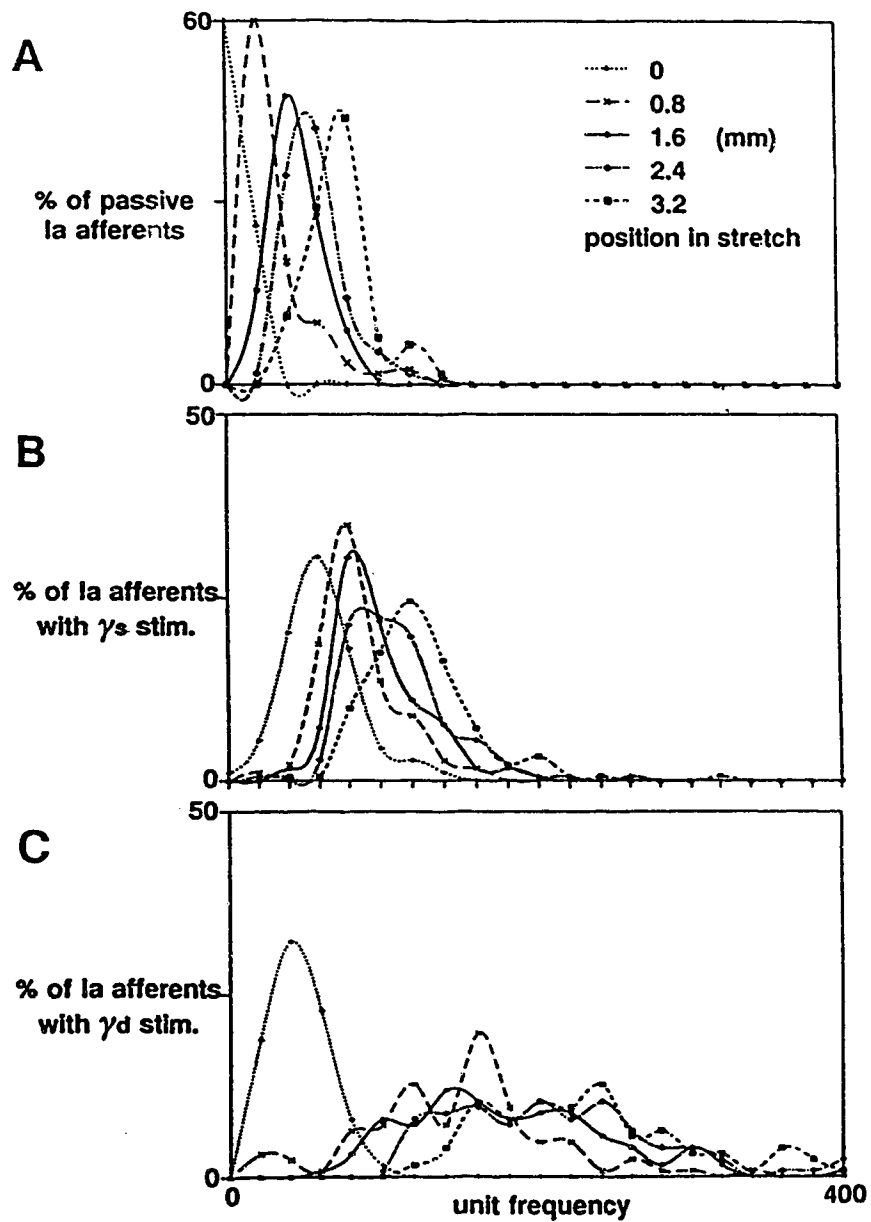


Figure 8 The effects of fusimotor activity on the distribution of firing rates seen in Ia afferents during a ramp stretch.

- A) Passive units.
- B) With γ_s stimulation at 100 ips.
- C) With γ_d stimulation at 100 ips.

Each line represents a different point in the same stretch (key in A common to all.)

Once the raw data were made available on the Olivetti systems the Extract program was written and used to obtain the instantaneous frequency of each unit at defined points in the ramp-and-hold cycle. This is shown in figure 7 where the mean frequency and ± 1 standard deviation (S.D.) bands are shown for the ramp. Due to the 3 point averaging used by Extract (see 2.3.1) the passive population showed a smeared acceleration component at the start of the ramp when compared to the other populations. Use of S.D. side bands to indicate the spread of a population is really only appropriate if the populations follow a true binomial distribution. The extent to which this is true can be seen in figure 8 where the distributions for 5 positions in the stretch have been plotted for each group and fitted with a polynomial curve. Notice in particular the large range of firing rates seen with γ_d stimulation once the stretch has started. The curves fitted with polynomials in figure 8 show that the passive and γ_s stimulated populations both have distributions that are slightly skewed, with more of the higher frequency units than low frequency ones. With the γ_d stimulation note the large range of firing rates once the stretch has started. Before the stretch (0 length) γ_d just shows a biasing effect similar to γ_s action. Once the stretch starts the distribution of firing rates becomes very broad due to the widely differing length and velocity sensitivities of the units while under γ_d stimulation.

These data on the population distributions were then used to generate the cumulative population curves in figure 9. Using this figure it was possible to build representative populations of any desired size with afferent characteristics typical of the whole range. This was done by dividing the y axis by the desired population size and then selecting the afferents firing at the frequencies given by the horizontal intercepts with the

Cumulative probabilities of Ia afferent firing rates
at six points in a ramp stretch.

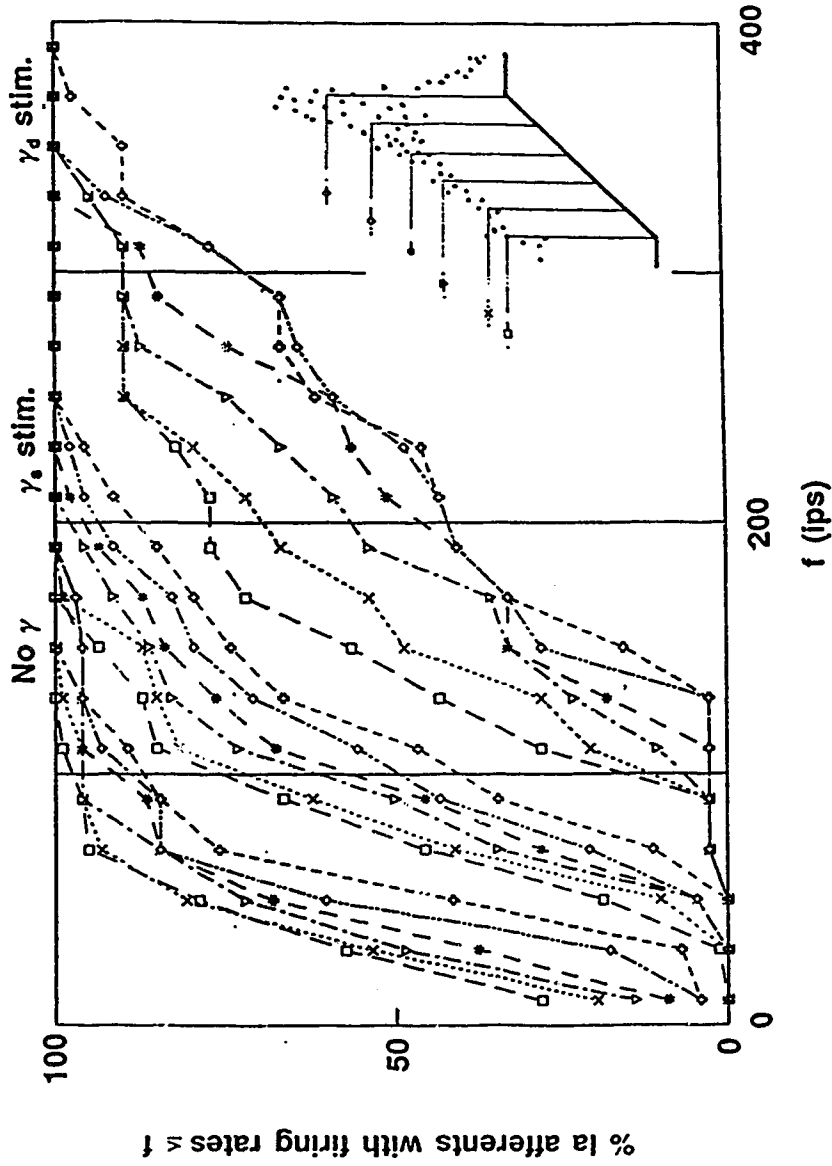


Figure 9 The cumulative probability functions used to assemble typical populations.

The frequency of each Ia afferent unit was taken at 6 places in the ramp stretch (see insert right) and combined to produce the cumulative probability curves left. Three different populations are shown. Passive, thick lines far left, with no γ stimulation. γ_e , thin lines centre, with identified static fusimotor drive. γ_d , thick lines on the right, identified dynamic fusimotor drive.

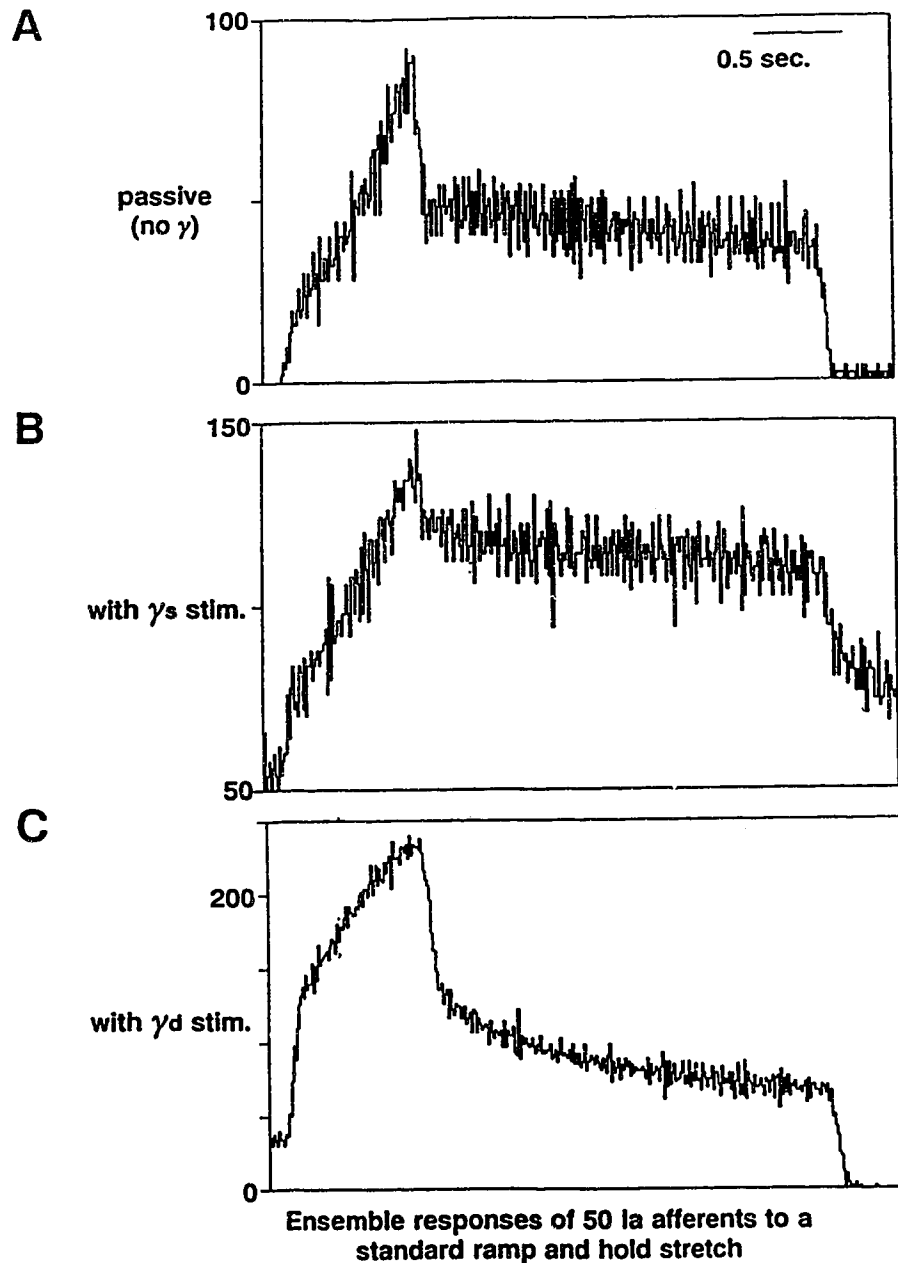


Figure 10 Ensemble responses of 50 Ia afferents to a standard ramp and hold stretch.

10 ms bin histograms constructed using populations of 50 Ia afferents during a ramp-and hold stretch. Each unit recorded separately and selected for the population of 50 on the bases of figure 9.

- A) Passive response without fusimotor activity.
- B) With 100 ips of static fusimotor stimulation added.
- C) With 100 ips of dynamic fusimotor stimulation added.

desired population curve. Using populations of 50 afferents selected in this way the afferent population spike trains (pdfs) were built up by Extract with a 1 ms bin width. With the 1 ms bin width the afferent firing rate was mostly indicated by the frequency of filled bins, not their height (for example see those in figure 5) so pdfs were also produced using a bin width of 10 ms. These are shown in figure 10 which shows the classic effects of fusimotor drive on Ia muscle afferents. The top panel (A) is the population of 50 afferents without any fusimotor drive. The passive population is silent during the pre-ramp phase, shows a dynamic jump to about 20 ips at the start of the stretch (acceleration component) and then increases to about 90 ips at the top of the stretch, followed by a fall of 40 ips (deceleration component, equivalent to the dynamic index for the population). During the hold phase the frequency falls slowly to about 35 ips. Most of the population again falls silent during the release phase. The effects of static fusimotor (γ_s) stimulation at 100 ips are shown in the middle frame (B). The firing rate of the population has been increased so that all 4 phases of the test signal can now be followed but the dynamic components have been reduced, the dynamic index being 15 ips, while the modulation depth during the stretch has not changed by very much (60 ips vs 70 ips). By comparison the dynamic fusimotor (γ_d) stimulation (C), also at 100 ips, causes a very large increase in both the dynamic (velocity) and static (length) sensitivity, the dynamic index being 85 ips while the change in firing rate during the stretch is nearly 80 ips with the peak firing rate reaching 230 ips. Notice also that the population shows some background activity during the pre-ramp phase but is totally shut off by the release phase (negative velocity). Similar histograms with a 1 ms bin width were used as the spike trains to be passed through the motoneuron model.

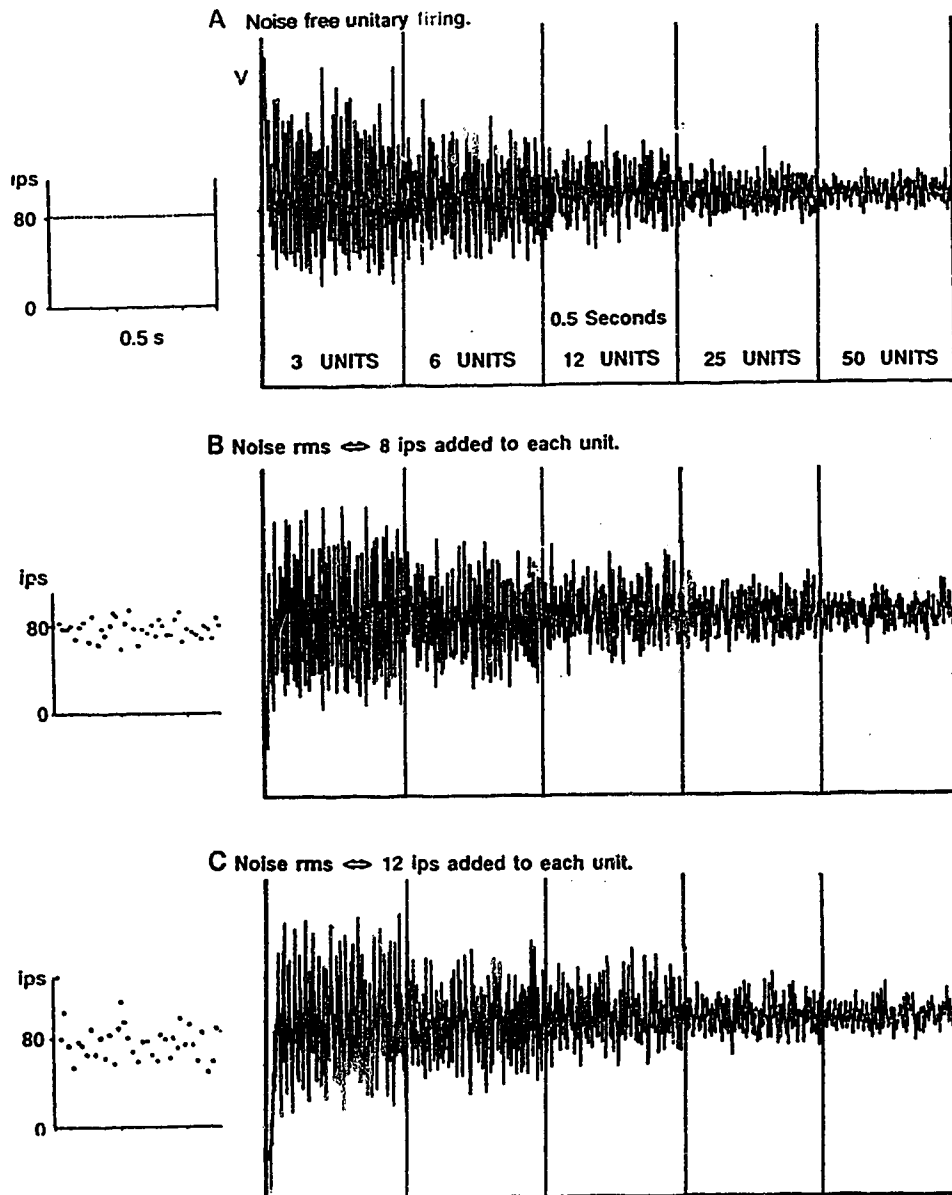


Figure 11 The effects of interspike variability on the motoneuron model.

- A) Populations of theoretical "carrier-noise free" afferents.
- B) Populations of afferents with carrier-noise corresponding to γ_s action.
- C) Populations of excessively noisy afferents. (Very high interspike variability).

Each population of units is based on the cumulative population curve of frequencies for γ_s stimulated units. Insets to the left are segments of firing of the median unit of each population. Each segment is 0.5 seconds long.

3.2 Modeled units

3.2.1 Effects of inter-spike variability and population size.

To investigate the effects of interspike variability and population size we took the spike trains built up using the VCO and noise generator and combined them into populations (see 2.2). The resulting pdfs were then played through the motoneuron model and short sections were digitised. These results are shown in figure 11. While few biological systems would be as clean as the unit shown in A and none of the actual populations were as noisy as that shown in C, the populations in 11B shows the level of noise appropriate for a population under γ_s drive. The effects of variability in firing frequency of individual units, as indicated by the inserts to the left, has very little effect on the variation in motoneuron membrane potential when compared to that caused by beating of the contributory frequencies from each afferent. The fluctuations caused by these beating effects can be reduced by increasing the mean firing rate or the numbers units contributing. The effectiveness of population size in reducing the distortion caused by noise is very clear from this figure.

The modeled membrane potentials were then used to calculate the signal to noise ratios (SNR) for these populations. Those with physiologically appropriate noise levels are shown in figure 12. Here it can be seen that as the stretch progresses the SNR improves slightly due to the increase in mean firing rate (more signal) but that fusimotor activity produces even greater gains in resolution despite the added noise in the form of interspike variability. In fact γ_s stimulation approximately doubles the resolution and γ_d quadruples

The signal to noise ratios of different sized populations of Ia afferents during a ramp stretch under different types of fusimotor drive.

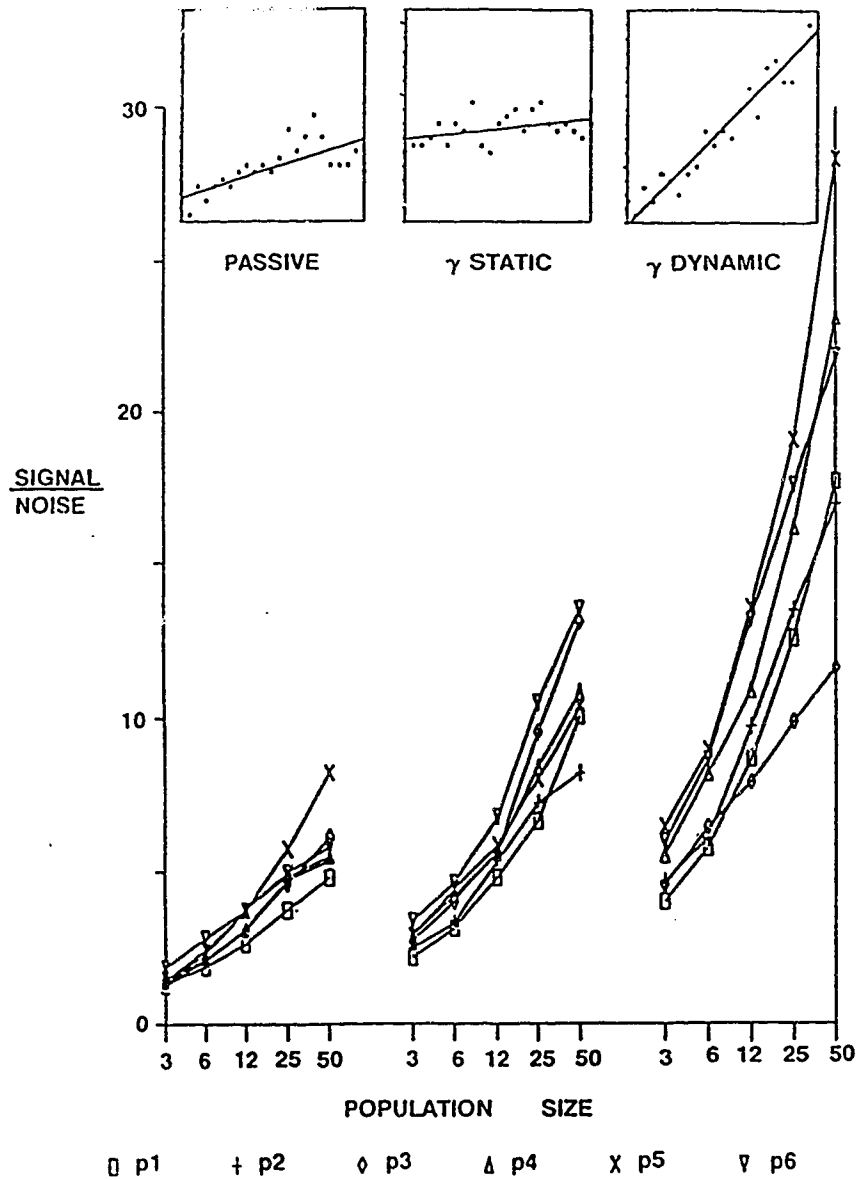


Figure 12 The signal to noise ratios of different sized populations of Ia afferents during a ramp stretch under different types of fusimotor drive. Typical single unit ramp responses inset at top. Position in ramp indicated by symbols in order p1 to p6. Passive population response (left), γ_s stimulated populations centre and γ_d stimulated population right. Increasing population size from left to right within group.

it. Changing the population size also improves the SNR, a population of 12 having about twice the resolution of a population of 3 and the populations of 50 double this again.

3.3 Recorded primary muscle afferents

3.3.1 Single units

With the library of real units it was then possible to look at the response of the model to actual firing patterns recorded by Dr. M. Hulliger. Figure 13 shows the typical response of a Ia muscle afferent to a ramp stretch with and without 100 ips stimulation to a single γ_d filament. From the instantaneous frequency plots in the middle the passive response appears to give the closest representation of the input signal. With γ_d stimulation the firing rate is highly variable near the peak. The model motoneuron membrane potential (lower traces) gives a very different impression. The passive response is extremely distorted by individual spikes. This is because the interspike interval is quite long when compared to the membrane time constant. With fusimotor action the overall frequency of firing and the depth of modulation both increase so that more EPSPs are integrated per unit time by the membrane to produce a response that looks much more like the original ramp profile.

3.3.2 Ensembles of primary muscle afferents

When the population responses were assembled and tested the results shown in figure 14 were obtained. To facilitate SNR comparisons, each of the responses have been normalized to produce similar maximum depolarization. The clear improvement in SNR due

Signal transmission by a Ia afferent to an α -motoneuron

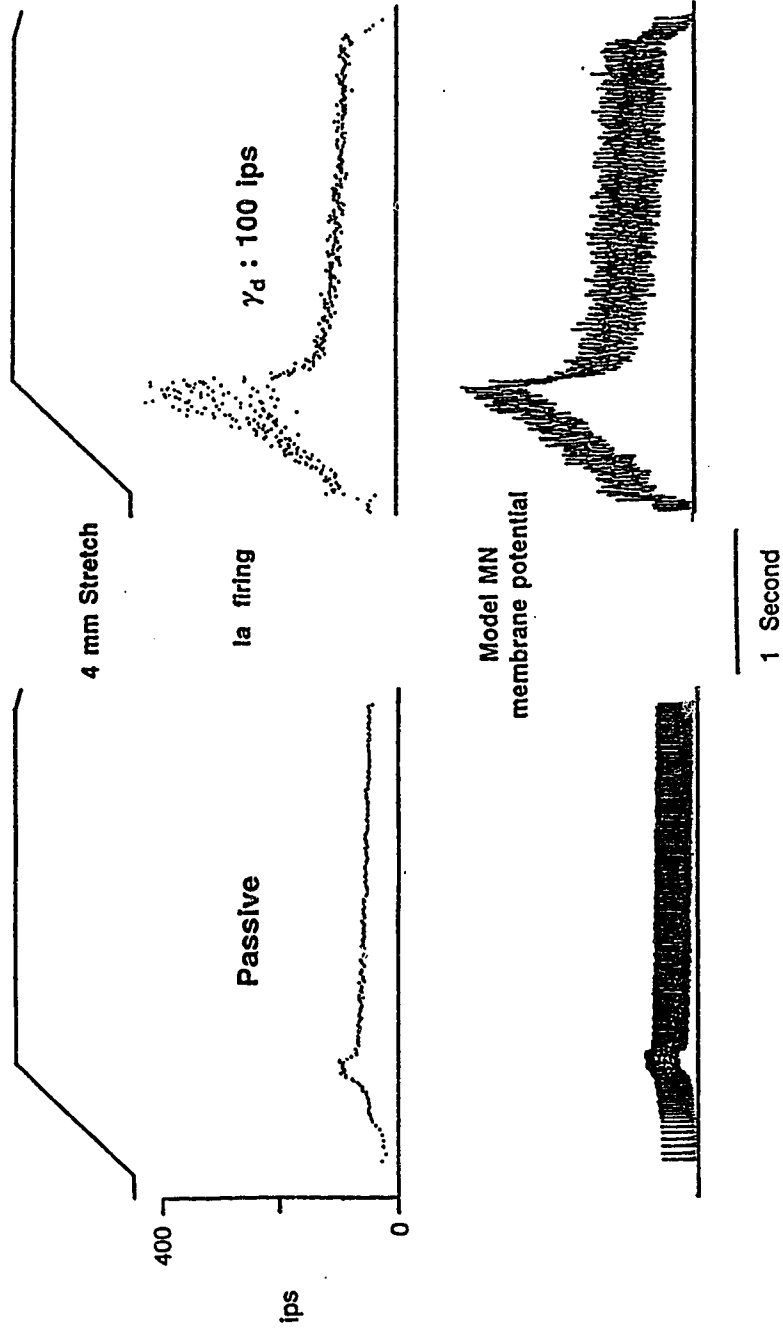


Figure 13 Signal transmission by a Ia afferent to an α -motoneuron.

The responses of a primary spindle afferent (centre) were recorded in response to the ramp-and-hold stretch (top). The recorded spike train was then passed through the motoneuron model to give the model membrane response bottom. The effect of adding γ_d stimulation is shown on the right.

RESOLUTION OF Ia ENSEMBLE RESPONSES

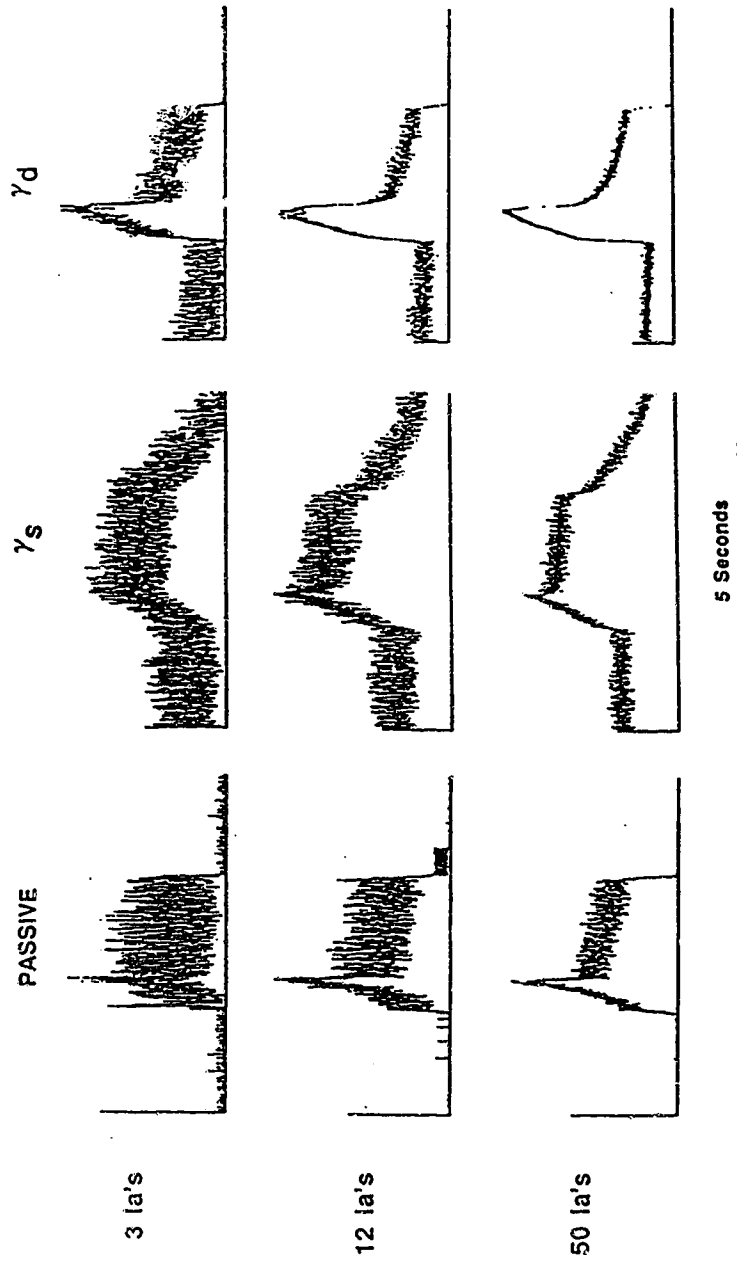


Figure 14 Resolution of Ia ensemble responses.

The Normalised response of the second order neurone model to the full ramp and hold test cycle is shown for 3 different population sizes.

Left column, Ia units responding passively to stretch. Centre column, Ia units with 100 ips of γ_s stimulation. Right column Ia units with 100 ips of γ_d stimulation. Note that it takes a population of 50 passive units to transmit the signal as well as a population of just 3 Ia afferents with γ_d stimulation.

to population size and fusimotor activity can be seen by comparing the top left trace (3 passive Ia units) with the bottom right trace (50 Ia units with 100 ips γ_d stimulation). As will be discussed later (section 4.10), these data show that similar fidelity can be achieved by different balances of population size and mean firing rate.

The concluding figure (15) shows the SNR against the equivalent mean firing rate for the population sizes of 3, 12 and 50 units. Each line is the SNR plotted against the instantaneous frequency for the ramp stretch between the initial and final dynamic phases. The γ_s stimulated units were left out of this plot since they just occluded the transition from the passive units to those stimulated by γ_d (on the overlay). The plots are very nonlinear but the general trend is for the SNR to increase with both mean firing rate and population size.

From this figure we calculated that a single Ia afferent firing at 95 ips (passive) gave 3 levels (1.6 bits) of discrimination instantaneously. A population of 50 such afferents (mean firing rate 95 ips) would increase this to 8 levels (3 bits) and the addition of γ_d stimulation would increase this value to 32 levels (5 bits).

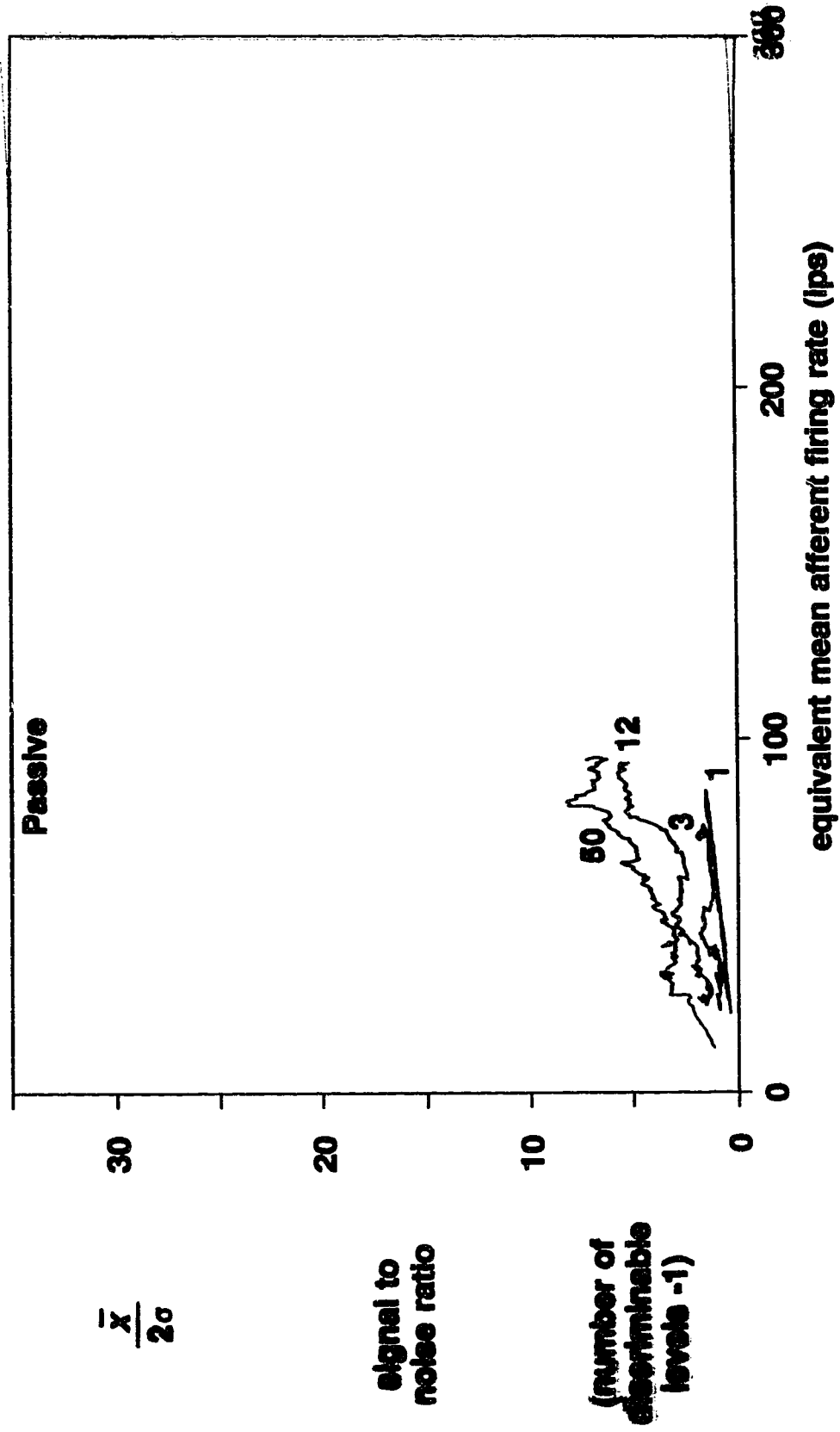


Figure 15a. Signal to noise ratio plotted against instantaneous mean frequency for populations of 50, 12, 3 and 1.

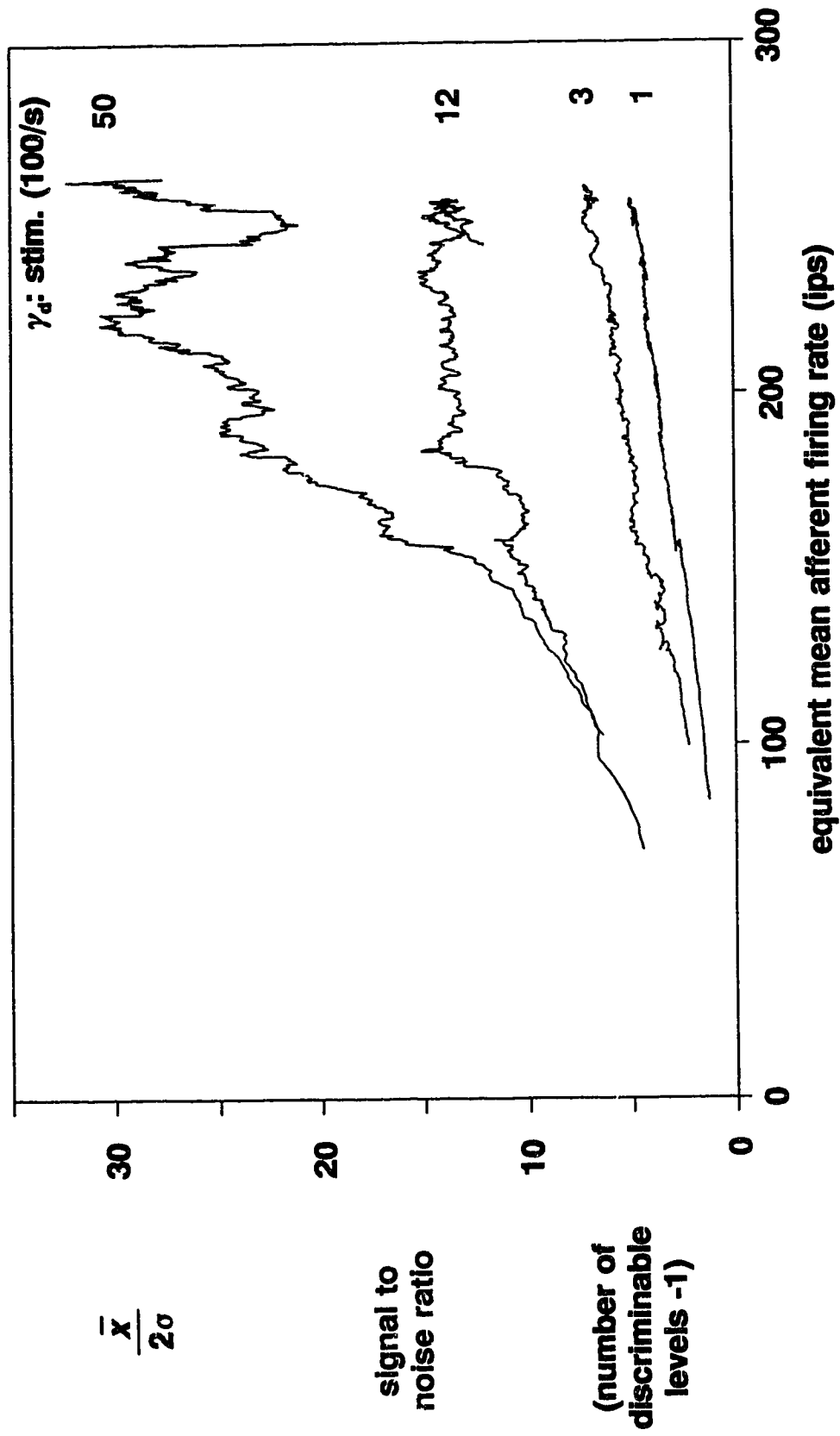


Figure 15b. Signal to noise ratio plotted against instantaneous mean frequency for populations of 50, 12, 3 and 1.

4 DISCUSSION

4.1 Neuronal ensembles

Throughout the central nervous system neurons exhibit wide fluctuations in firing behaviour. In many cases this fluctuation is dependent on the state of the animal under study, a sleeping subject will exhibit much lower levels of mass neuronal activity than a highly agitated one (Moruzzi and Magoun, 1949). From section 1.4 we have shown that each action potential has a finite cost. So what is gained by the added expenditure of higher firing rates? The muscle proprioceptive system, in which state-dependent changes in firing rate occur (Prochazka, 1989b), provides a well studied and accessible system in which to investigate this question. A large data base of afferent firing patterns collected over a period of 10 years by Dr. M. Hulliger provided us with possibly the most complete set of data available on any discrete neuronal system with which to analyze the characteristics of large ensembles. This has allowed us to characterise the firing behaviour of the muscle Ia afferent pool under different conditions of fusimotor drive during test ramp-and-hold signals under acute conditions and relate this to the normal behaviour of chronically implanted cats (Prochazka et al, 1985, 1988).

Prior to the present work, there have been several other studies of the net activity or post-synaptic action of neural populations. For example, Joffroy (1975) and his co-workers have attempted to discriminate the activity of discrete populations of neurones in

peripheral nerves by their mass effects and from recordings of the whole nerve. A sophisticated signal processing system was used to separate afferent and efferent action potentials by conduction direction and velocity. Using this method Bessou et al (1989) have attempted to study fusimotor activity during walking in thalamic cats. Unfortunately, the method is unable to separate γ_d and γ_s activity, the effects of which can be very different, or Ia (primary muscle spindle) and Ib (Golgi tendon organ) afferents, the activities of which are out of phase during slow walking (See Prochazka et al, 1989). Another approach has been to record the effect of afferent populations on motoneurons intracellularly in decerebrate cats (Poppele and Terzuolo, 1968). Sinusoidal fluctuations in membrane potential were detected in response to imposed sinusoidal movements without averaging. While this shows that the motoneuron membrane potential can follow the imposed muscle length changes, the exact nature of the afferent population involved is unknown. In addition to primary muscle afferents, other afferents could have contributed, via either mono- or poly-synaptic pathways, so the input cannot be considered as having been from a single identified afferent population.

In the cerebral cortex both Fetz and Georgopoulos have studied populations of neurons with respect to movement by combining the responses of individual units into ensembles. Georgopoulos (1988) proposed that the direction of a voluntary movement is coded by the whole population of directionally-sensitive neurons in the motor cortex, with each cell's firing rate being dependent on the cosine of the angle between the actual movement direction and the cell's preferred direction. Recording from cortico-motoneuronal (CM) cells, Fetz et al (1989) produces an estimate of the firing pattern of the whole population by combining the responses of the different categories of CM cells, weighted

according to their frequency, and related this to the recorded electromyogram (emg) and force output of the muscle that these CM cells project to. As with Georgopoulos, the information (in this case muscle activity rather than direction) is transmitted by the whole population and not individual units.

The emg provides an easily recorded record of the activity in a single population of efferent units. Using emg recordings it has been possible to build up profiles of coordinated muscle activity during normal movements (for example see figure 1 of Prochazka *et al.*, 1989). These charts provide a clear indication of the efferent output from the nervous system in a task-related manner. While the net output of this system is known the actual command input is not. Furthermore, as far as we know, the net firing rate profiles of ensembles of motor units have not been analyzed.

None of these studies show what is gained by the combination of the units into population or how the changes in firing rate benefit the animal compared to the use of single sensors.

4.2 Quantitative information on Ia afferent behaviour

Figures 6 to 9 show how the distribution of unit firing frequency changes with stretch and fusimotor stimulation. As was expected from the behaviour of single muscle afferents (for review see Matthews, 1972), both stretch and fusimotor stimulation increased the mean afferent firing rate. In particular the effect of dynamic fusimotor stimulation is predominantly a change in stretch sensitivity (or dynamic index) of each unit (figure 7).

γ_d action also increases the resting firing rate of Ia afferents (bias), although not as strongly as does γ_s action. This can be seen by comparing the zero length distributions in figure 8 for the populations with γ_d or γ_s fusimotor drive with the passive population, both types of fusimotor drive produce similar distributions of firing rate but the γ_s drive has a higher mean. Once the stretch starts the similarity is lost and the γ_d stimulated populations becomes spread over a far wider range of frequencies. By comparison γ_s stimulation increases the "bias" firing rate of each unit while the stretch and acceleration sensitivity of the population is slightly reduced. The reduction in stretch sensitivity can be seen clearly in figure 7 while the reduction in dynamic sensitivity is best shown in figure 10 and with the filtered ensemble responses of figure 14. This produces an ensemble response that follows the input ramp-and-hold much more closely throughout the cycle than the passive or γ_d populations with maintained firing during shortening and with reduced velocity sensitivity. In addition to the predicted changes in behaviour of individual units the population as a whole shows that increases in firing rate are associated with a broadening of the range of firing rates. In particular γ_d stimulation produces a very broad range of firing rates but both the γ_s and passive populations show some widening distribution with increased mean frequency (see figure 8).

4.3 Cumulative data enables the construction of typical populations

The final figures of this section (9 and 10) provide a clear indication of the spread of behaviour of individual afferents under the two kinds of fusimotor drive and how these different units combine to produce ensemble inputs to the C.N.S. Figure 9 enables the behaviour of any Ia afferent to be characterized with respect to the population. With this

it was possible to construct hypothetical populations representative of the ensemble input to the spinal cord by the Ia afferent population of muscles of differing spindle content.

Figure 10 is such a representation and shows how γ_s and γ_d drive both change the characteristics of the transduced signal. These figures have been normalised and show how the higher firing rates under γ_d drive provide a much "cleaner" signal during the stretch phase. In the latter part of the "hold" phase, the SNR is actually better with γ_s stimulation (i.e. mean rate/variance is greatest). The dynamic responses are clearly different for γ_s and γ_d action as expected from the literature (Matthews, 1972) and the nature of the transmitted signal and the role of the dynamic components will be discussed later (See 4.4). While this figure was constructed with a relatively arbitrary 10 ms bin width used for illustrative purposes, the actual ensemble input received by the spinal cord is a barrage of action potentials, each producing unitary EPSPs in motoneurons that last about 6 ms (average of time to peak and decay time, Table 3 Burke, 1967) which are integrated by the receiving neurons. When combined with studies on EPSP size (e.g. Burke, 1967, Kirkwood and Sears, 1982, and Redman and Walmsley, 1981) and the connectivity of muscle afferents to motoneurons (Fleshman et al, 1981 and Clamann et al, 1985) it is possible to estimate the net effects of the spindle afferent pool on the motoneuron pool (Prochazka, 1989a). Even without this information the force frequency relationship (0.03 N/Hz above 50 Hz), developed by Matthews (1966) in a decerebrate cat, suggests that we might expect 1 N of reflex force in the soleus muscle at the peak of the stretch and gamma activity could increase this to 2.7 N (γ_s) or 5.7 N (γ_d).

4.4 Dynamic components of response: signal or noise ?

Throughout this thesis the noise values of our signals have been calculated from the variability of the signal about the local mean depolarization. Comparison of the actual input signal (the original ramp-and-hold length change) with the output signal (the membrane potential) shows that the output signal deviates substantially in the response at three points; the start of the stretch, the end of the stretch and the start of the release (particularly with γ_s drive, see the right hand side of figure 13). These step changes are due to the velocity component of sensitivity of the spindle primary and if the role of the spindle was purely that of a length transducer these components would represent noise or distortion components. However there are various reasons for believing that velocity components of the spindle do represent useful elements of signal. For example, in the reflex arc, velocity sensitivity may serve to stabilize the control loop (Poppele and Terzuolo, 1968, Roberts *et al.*, 1971), or to linearize muscle properties (Stein and Oğuztöreli, 1976). In most man-made feedback control systems dynamic response characteristics are deliberately incorporated in the feedback pathway to rapidly counteract external perturbations and to avoid instability at high loop gain.

Fusimotor action affects these two feedback components in different ways (See Matthews, 1972). γ_s stimulation increases the mean firing rate ('bias') of each unit and reduces the velocity sensitivity, this means that the transmitted signal is more closely related to the length changes of the muscle than the pure passive response. γ_d stimulation produces a somewhat smaller increase in mean firing rate and also large increases in the velocity sensitivity of each unit.

Figure 10 shows how fusimotor drive can increase the resolution of the transduced signal; it also shows how fusimotor activity increases the cost. The 50 passive Ia afferents in Figure 10A transmitted a total of 7,011 action potentials in the segment shown (3.25 s). Fusimotor activity (Figure 10B and C) nearly tripled the corresponding number of action potential (totals of 18,698 (γ_d) and 20,607 (γ_s)). The energy cost with the static fusimotor drive was highest since the bias was maintained during the hold and release phases. The γ_d expenditure was concentrated during the stretch phase of the signal. Recordings in conscious cats have led to the proposal that γ_s action increases with increased activity (stance, slow walk, fast walk) while the γ_d system is activated for novel or unpredictable tasks (Prochazka *et al.*, 1985 and 1988). At least for balancing and imposed movements it is to be expected that accurate and sensitive knowledge of any changes occurring would be more important than the actual position.

4.5 Predictions from mathematical analysis

In this thesis we have looked at the effects of changing population size and fusimotor activity on the transmission of proprioceptive information to the motoneurons. Stein (1967b) studied the information capacity of nerve cells using a frequency code by using different statistical models of the randomness in each channel. He has suggested that the information content of the system should increase according to the formula $0.5 \log_2 (Nt)$ where N is the population size and t the time period investigated. In his study the carrier frequency and modulation depth were fixed. From this formula it is predicted that increasing the population increases the SNR by the square root of the population size. Increasing the sampling period t will also increase the SNR as the square root of t .

Increasing the mean frequency of the population will also affect the SNR since more action potentials will be transmitted per unit time and this will have the same effect as increasing the time t . The equation also suggests that population size, unit frequency and sampling period may be traded off against each other and that the expected information capacity varies as the square root of the product of these three elements. In other words the same net number of action potentials per second should produce the same SNR whether from a single high frequency unit or lots of low frequency units.

However, spectral analyses and modelling of IPFM led to other predictions regarding the effect of changing these parameters. Bayly (1968) found that, for a system using IPFM, increasing the number of parallel channels should directly increase the SNR (i.e. increasing the population by 10 should improve the SNR by 10) if the channels have non-identical carrier rates and that even for identical carrier rates an improvement will be seen as long as the channels are not in phase with each other. Milgram and Inbar (1976) used computer modelling techniques to apply the work of Bayly (1968) and Lee and Milsum (1971) to the afferent limb of the mono-synaptic reflex. They showed that the SNR did improve in direct proportion to the population size if each channel had a different firing threshold (which would meet the requirement of Bayly for differences in phase). In addition the introduction of differences in threshold within as well as between channels produced a near optimal transmission of phasic information. Milgram and Inbar concluded by suggesting that "by increasing the level of fusimotor excitation of the muscle spindle's, both the degree of interchannel threshold randomness and the average levels of muscle spindle activity should increase correspondingly, enhancing the range of frequencies which can be transmitted effectively, and thus increasing the system's bandwidth and gain."

Since we are using a fixed low pass filter with a 20 dB per decade roll off we can also predict that increasing the carrier frequency by 10 should reduce the associated noise components by 10 while the signal components are below the filter cut off frequency and so will not be effected (figure 1).

The effects of fusimotor activity on the population will be to: 1) Decrease each unit's initial threshold. 2) Increase the spread of firing thresholds in the population. 3) Increase the dispersion of carrier rates within the population. 4) Increase the effective carrier rate of each unit (especially for γ_s activity). 5) Increase interspike variability. Of these five actions we expect from all of the above that an improvement in SNR would be produced by the first 4 actions while 5 would reduce the SNR. Action 1 would increase the effective population size by bringing in more units (% percent of the population firing), 2 and 3 would improve the SNR by dispersing the noise components while 3 will increase the carrier frequency of each unit.

To summarise;

- 1) Increasing the population size was predicted to improve the SNR either in proportion to the population size or its square root (Bayly, 1968 or Stein, 1967b). My results supported this relationship.
- 2) Stretching improves the SNR by increasing the firing rate of each unit (seen in figures 7 12 and 15).

- 3) Fusimotor activity improves the SNR by; a) increasing the dispersion of firing thresholds within the afferent population (as suggested by Milgram and Inbar, 1976), b) increasing the dispersion of carrier rates (Bayly, 1968, this is seen in figure 8), c) increasing the number of action potentials received per unit time (increased carrier frequency, Stein, 1967b. See figures 9,10 and 15) and d) increasing the separation between the carrier rate of each unit and the filter cut of frequency (Bayly, 1968). The increase in interspike variability may reduce or increase the SNR depending on the signal frequency components (Stein and French, 1970) and the presence or absence of temporal correlations between afferent spike trains (Stein, 1967b, Inbar et al, 1979).
- 4) In addition γ_d stimulation will increase the modulation depth which will further increase resolution.

4.6 Smoothing effects of the motoneuron model.

When an action potential influences a post-synaptic cell the effects of chemical transmission and the capacitance of the receiving membrane is to low-pass filter the sharp action potential into a longer, smaller EPSP. Since each motoneuron receives input from many afferents the EPSPs are integrated, each one causing a small fluctuation in the membrane potential. Figure 11 shows how the numbers of afferents involved affect the size of this fluctuation. This figure has been normalised so that each population produced the same net depolarization of the modelled membrane. Each population represented the total spindle afferent input to the target motoneuron.

We have chosen not to model the onward transmission of the information in terms of motoneuron firing since this will involve the additional facilitatory and inhibitory inputs from other, particularly descending, systems about which we had little information. In addition the subsequent encoding of the input signal for transmission to a third cell will, in many cases, be dependent on the nature of the target. For instance, while both motoneurons and DSCT cells receive input from Ia afferents the former, transmitting information to another neuron, may fire at nearly 1000 ips (Kuno and Miyahara, 1968) while for the motoneuron the range of firing rates produced are matched to the type of muscle fibre innervated (Kernell, 1983) and rarely maintain 30 ips with short initial bursts reaching 120 ips (Freund, 1983).

4.7 The effects of synchronisation between muscle afferent discharges.

If there was a tight temporal synchrony between spike trains of the muscle afferent population of a normal animal this would have the effect of reducing the effective population size. Since each afferent was recorded independently any such correlation would have been lost. This synchrony could be induced due to a) common or synchronous fusimotor activity, b) unfused motor activity in series with the afferents, c) blood pressure or other mechanical artifacts or d) external disturbances such as vibration. The correlations found are relatively broad (due to the relatively slow time constants of factors a-c compared to the mean EPSP duration of about 6 ms, see 4.3) and can be both negative or positive (Windhorst 2.5-2.7 1988). The effect of these correlations on the motoneuron is not totally clear but for the population as a whole the presence of both positive and negative correlations and the relatively broad peaks would indicate that tight correlations between

multiple afferents causing reliable large composite EPSPs do not normally occur, though in unusual circumstances such as the presence of external vibration, or during very rapid displacements such as those in shivering tremor, some synchrony would be expected.

4.8 Interspike variability.

Matthews and Stein (1969) suggested that the addition of interspike variability by fusimotor activity reduced the resolution of a single primary afferent from 28 to 6 discriminable levels measured over 1 second. By modelling the effects of interspike variation on the transmission of information Stein and French (1970) showed that while the variability reduced the resolution at all frequencies and at the high end in particular, it also extended the linear range and reduced distortions due to phase locking.

In figure 11 the variability in the membrane potential is virtually identical in A, B and C despite the large differences in the r.m.s noise added to the contributing afferent firing patterns. This is because of the low pass filtering and integrating effect of the membrane time constant. This is even shown by the single units passed through the model in figure 13 where the high scatter of the γ_d stimulated unit on the right is lost in the motoneuron membrane response bottom right while the relatively steady but slow firing rate of the passive unit (left) produces a series of partially-fused EPSPs in the modeled motoneuron bottom left. Thus, any increase in interspike variability caused by fusimotor action has little effect on the SNR measured at the motoneuron membrane, in contrast to the improvement resulting from the increase in mean frequency. This implies that the SNR is dependent on the net firing rate of the afferent population and is little affected by the

interspike variability of individual units. If there is any correlation between the firing of passive afferents the addition of fusimotor-induced interspike variability will tend to remove this and result in a further improvement in SNR.

4.9 Implications from modelled units

From the modelled unit data (figure 11) it can be seen that the resolution of the transmitted signal is dependent on the numbers of contributing units and adding noise in the form of interspike variability has little effect on the signal as received by the putative motoneuron. In this figure the induced noise is very small compared to the fluctuations in membrane potential caused by the arrival of individual spikes. These fluctuations are only smoothed by the increased net rate and smaller EPSP size associated with the larger populations. In figure 12 the responses of the different modelled populations are shown. For all the populations there is an improvement in the SNR with increasing length but this is small compared to the improvement due to fusimotor action or increased population size. The γ_d populations gave the best resolutions, as would be expected during a phasic input, producing deeply modulated firing and a wide range of carrier rates.

4.10 Implications from assembled populations

From figures 14 and 15 we can see that the signal resolution is dependent on the population mean carrier rate and the number of units in the population. Figure 15 plots the resolution against the mean firing rate for the population. This shows that the SNR does increase with population size and mean firing rate within the population as expected.

When the same net rates are achieved in different populations they do not produce the same resolution. For example in figure 15 a population of 12 Ia afferents with fusimotor stimulation firing at 200 ips gives a far better resolution than the population of 50 Ia afferents without γ action firing at 50 ips (a net rate of about 2.5 Kips in both cases). This improvement in resolution with higher frequencies indicates that the equation $0.5 \log_2 (Nt)$ is too simple to predict the improvement in resolution expected from fusimotor activity especially when the multiplicity of factors affected by fusimotor action (See page 56) are considered.

4.11 Effect of population size

With figures 12, 14 and 15 we see that population size (affecting net firing rate), fusimotor drive and mean firing rate all affect the achievable resolution. Figure 12 shows for the original modelled units how stretch, population size, and the power of fusimotor action all act to raise the SNR at the motoneuron. With the modeled neurones the results show a small amount of improvement due to the increased firing rate from stretch.

Figure 14 shows the motoneuron response to the different ensembles of afferent units. The comparison from top right to bottom left is particularly informative, in that a population of 50 passive afferents gives only a slightly better representation during the stretch than the 3 Ia units with γ_d drive. To achieve this it uses many more action potentials (50×50 compared to 3×250 based on figure 9), and so involves a far higher cost. This is also illustrated by comparing the 12 Ia units with γ_d drive (middle right) with the 50 passive units (bottom left). The 12 units give a slightly better SNR than the 50 units

even though the net firing rates in the two were quite similar ($50 \times 50 = 2500$ vs $12 \times 250 = 3000$ impulses). Fusimotor activity therefore improves the resolution of the received signal by increasing the net firing rate so that each unit can do the work of four. If this is true, and the passive firing rates are representative of the sustainable rates, then the fusimotor system reduces the number of passive afferents needed by a factor of four. Since the muscle afferents are all large (group I) fibres this would represent a significant saving in nerve bulk. Of course the afferents, in the absence of a fusimotor system, could have higher sustainable and mean firing rates but we have seen from 1.4 that this has its own price.

The final figure (15) shows how the SNR's improve with the increasing length and fusimotor action (left to right) and with population size. With a single passive unit there is a small increase in resolution due to the increased firing rate of the unit caused by the stretch. The addition of more units, selected on the bases of figure 9 to form an ensemble, increases the resolution at any mean rate and the rate of improvement with increased firing rate. Fusimotor stimulation (in particular γ_d) extends the range of frequencies over which each afferent fires and shifts that range towards higher firing rates. This combines to raise the resolution. Multiple units with gamma action combined also have the effect of increasing the slope of the SNR vs frequency relationship. This improvement effect of multiple units was expected to some extent as Stein (1967b) suggested that a population of N afferents should transmit $0.5 \log_2(N)$ times as much information, expressed in bits, as a single unit. The actual populations used for figure 15 gives an estimated improvement of $0.46 \log_2(N)$, a fairly close agreement. By comparison the improvement due to increasing firing rate is far larger than would be expected from the relationship $0.5 \log_2(t)$.

The γ_d lines are almost continuations of the passive lines and this indicates that the achieved resolution in each population is directly related to the mean firing rate. Any "contamination" due to increased variability being of negligible effect on the second order neurone. The size of the contributing population is the other contributing factor, larger populations achieving information capacities dependent on the square root of population size.

4.12 Other target neurones

While the mammalian monosynaptic reflex connection is one of the most studied and best understood it is always useful to try to generalize. The Ia afferents we have studied also project to relay cells of the DSCT (In Clark's column for hindlimb afferents and nucleus Z of Landgren and Silfvenus (1971) for forelimb afferents) and other interneuronal systems. Of these only the DSCT cells in Clark's column have been studied in any detail. Each DSCT cell only receives about 12 to 16 muscle afferents (Eide, 1969) but each afferent produces a much larger and briefer EPSP than in motoneurons (Walmsley, 1989) indicating that the synapses are much closer to the soma. It is tempting to suggest that the input to these DSCT cells would be equivalent to the 12 unit sized populations compared to the 50 unit populations going to the motoneurons. While the effect of the shorter EPSP times would be to reduce the effective population size, compared to our model, the longer membrane time constants (5.9 - 18.2 ms, mean 10.9 ms Walmsley, 1989) would counteract this to some extent. Unfortunately, somatic synapses are known to interact and the EPSPs in DSCT cells do not always sum algebraically so the comparison is somewhat limited.

For other systems the simple integration of all the sensory input may not be appropriate. For instance in the somatosensory area of the cortex, not only are the cells excited by the sensory endings within their receptive field they are also inhibited by the sensors surrounding that field, so some of the information must undergo a sign change. Alternatively synaptic input may induce long term changes in the post-synaptic neuron, for example the Purkinje cells of the cerebellum receive input from a climbing fibre which induces a complex spike in the Purkinje cell. When these complex spikes are combined with the simple spikes from mossy fibre input the result is a change in the subsequent synaptic efficacy of the mossy fibre input (Ito, 1984).

5 CONCLUSIONS

The purpose of this work was to investigate the costs and benefits of large populations of neurons and / or high firing rates for the transmission of information in the nervous system. The review of the literature on the cost of neuronal activity indicated that the major limitation relating to high firing rates is the availability of transmitter in a releasable form. Even at quite moderate firing rates transmitter replacement can not keep up, but by using internal stores neurons are able to fire at higher rates for a while. The debt incurred must eventually be repaid.

It was found that the low-pass filtering characteristics of the motoneuron model greatly reduced the "noisiness" seen when compared to the instantaneous frequencygram of the contributing afferent. When ensembles were used, even better SNR's were obtained. As the population size increased so did the SNR and this data was in agreement with the proposal of Stein (1967b) that the information carried by a population of neurons is approximately equal to the mean information carried by one neuron multiplied by the square root of the number of neurons. We were surprised to find that the SNR was not uniquely determined by net ensemble firing rate. A better SNR was obtained for the same net rate from a small ensemble with a high mean firing rate than from a large ensemble with a low mean firing rate.

Static fusimotor (γ_s) stimulation improved SNR by increasing the mean firing rate (bias) of the population. The increased bias was surprisingly costly in the sense that the

total number of action potentials over the whole stretch sequence was higher for γ_s action than for dynamic fusimotor (γ_d) action. γ_d stimulation improved the SNR only during stretch because this was where the mean carrier rates (and modulation depth) were greatly elevated. During shortening, pure γ_d action did not maintain firing so no information was transmitted. Thus γ_d action resulted in greatly enhanced information transmission (and cost) for the stretch phase, but a lower cost averaged over the full cycle.

The fusimotor system, by increasing Ia firing rates, can approximately quadruple the resolution of proprioceptive information reaching the motoneuron. From section 4.11 above it would require a 16 fold increase in population size to achieve this same resolution with units firing in the passive range. We therefore inferred that by using the fusimotor system to drive the afferent neurones in a higher frequency range during critical periods the nervous system could obtain the benefits of high net firing rates without carrying the cost of maintaining a larger population of neurones able to provide the same net rate continuously. The metabolic debts thus incurred would have to be repaid during periods of low neuronal activity.

REFERENCES

Ash, R, 1965 Information Theory. Interscience publishers, John Wiley & Sons, New York.

Band, D.M. and Wolff, C.B. 1978 Respiratory oscillations in discharge frequency of chemoreceptor afferents in sinus nerve of anaesthetized cats at normal and low arterial oxygen tensions. Journal of Physiology 282 pages 1-6.

Bayly, E.J., 1968 Spectral Analysis of Pulse frequency modulation in the nervous system. IEEE Transactions on Biomedical Engineering. BMED 4 pages 257-265.

Bessou, P., Dupui, Ph., Cabelguen, J.M., Joffroy, M., Montoya, R. and Pagès, B. 1989 Discharge patterns of γ motoneuron populations of extensor and flexor hindlimb muscles during walking in the thalamic cat. In Progress in Brain Research 80 Eds Allum, J.H.J and Hulliger, M., Amsterdam: Elsevier pages 37-45.

Birks, R., and MacIntosh, F.C., 1961 Acetylcholine metabolism of the sympathetic ganglion. Canadian Journal of Biochemistry and Physiology 39 pages 787-827.

Brink, F., Jr., Bronk D.W., Carlson, F.D., and Connelly, C.M., 1952 The oxygen uptake of active axons. Cold Spring Harbour Symposium on quantitative Biology 17 pages 53-67.

Burke, R.E., 1967 Composite nature of the monosynaptic excitatory postsynaptic potential. Journal of Neurophysiology 30 pages 1114-1137.

Capek, R., Esplin, D. W., and Salehmoghaddam 1971 Rates of transmitter turnover at the frog neuromuscular junction estimated by electrophysiological techniques. Journal of Neurophysiology 34 pages 831-841.

Ceccarelli, B. and Hurlbut, W.P. 1975 The effects of prolonged repetitive stimulation in hemicholinium on the frog neuromuscular junction. Journal of Physiology 247 pages 163-188.

Ceccarelli, B., Hurlbut, W.P., and Mauro, A., 1973 Turnover of transmitter and synaptic vesicles at the frog neuromuscular junction. The Journal of Cell Biology 57 pages 499-524.

Clamann, H.P., Henneman, E., Lüscher, H.R., and Mathis, J. (1985) Structural and topographical influences on functional connectivity in spinal monosynaptic reflex arcs in the cat. Journal of Physiology 358 pages 483-507.

Connelly, C.M., 1959 Recovery processes and metabolism of nerve Reviews of modern physics 31 #2 pages 475-484.

Curtis, D.A., Eccles, J.C., and Lundberg, A., 1958 Intracellular recording from cells in Clark's column Acta Physiologica Scandinavia. 43 pages 303-314.

Eccles, J.C., Oscarsson, O., and Willis, W.D., 1961 Synaptic action of group I and II afferent fibres of muscle on cells of the dorsal spino-cerebellar tract Journal Physiology 158 pages 517-543.

Eide, E., Fedina, L., Jansen, J., Lundberg, A., and Vyklicky, L. 1969 Unitary components in the activation of Clark's column neurones. Acta Physiologica Scandinavia. 77 pages 145-158.

Emonet-Dénand, F., Laporte, Y., Matthews, P.B.C., and Petit, J., 1977 On the subdivision of static and dynamic fusimotor actions on the primary ending of the cat muscle spindle. Journal of Physiology 268 pages 827-861.

Esplin, D.W., and Zablocka-Esplin, B., 1971 Rates of transmitter turnover in spinal monosynaptic pathway investigated by electrophysiological techniques. Journal of Neurophysiology. 34 pages 842-859.

Fetz, E.E. Cheney, P.D. Mewes, K. & Palmer, S. (1989) Control of forelimb muscle activity by populations of corticomotoneuronal and rubromotoneuronal cells. In: Afferent Control of Posture and Locomotion. Editors. Allum, J.H.J. & Hulliger, M. Progress in Brain Research. Amsterdam: Elsevier.

Fleshman, J.W., Munson, J.B. and Sybert, G.W. (1981) Homonymous projection of individual Group Ia-fibres to physiologically characterized medial gastrocnemius MNs in the cat. Journal of Neurophysiology 46 pages 1339-1348.

Freund, HJ. 1983 Motor unit and muscle activity in voluntary motor control. Physiological Reviews 63 pages 387-436.

Georgopoulos, A.P. 1988 Neural integration of movement: role of motor cortex in reaching. The FASEB Journal 2 #13 pages 2849-2857.

Granit, R., Kernell, D., and Lamarre, Y., 1966a Algebraical summation in synaptic activation of motoneurons firing within the "primary range" to injected current Journal of Physiology 187 pages 379-399.

Granit, R., Kernell, D., and Lamarre, Y., 1966b Synaptic stimulation superimposed on motoneurons firing in the "secondary range" to injected current Journal of Physiology 187 pages 401-415.

Greengard, P., and Straub, R.W., 1959 Effect of frequency of electrical stimulation on the concentration of intermediary metabolites in mammalian non-myelinated fibres. Journal of Physiology 148 pages 353-361.

Inbar, G., Madrid, J., and Rudomín, P., 1979 The influence of the gamma system on cross-correlated activity of Ia muscle spindles and its relation to information transmission. Neuroscience Letters 13 pages 73-78.

Ito, M. 1984 The modifiable neuronal network of the cerebellum. Japanese Journal of Physiology. 34 pages 781-792.

Jack, J.J.B., Miller, S., Porter, R., & Redman, S.J., 1970 The distribution of group Ia synapses on Lumbosacral spinal motoneurons in the cat. In Excitatory Synaptic Mechanisms Eds P. Andersen and J.K.S., Jansen, pages 199-205.

Joffroy, M. (1975) Méthode de discrimination des potentiels unitaires constituant l'activité complexe d'un filet nerveux non sectionné. Journal of Physiology (Paris) 70 pages 239-252.

Kernell, D. 1983 Functional properties of spinal motoneurons and gradation of muscle force. In Motor control mechanisms in health and disease. Ed. J.E. Desmedt, Raven Press, New York.

Kernell, D., 1983 Functional properties of spinal motoneurons and gradation of muscle force. In: Motor Control Mechanisms in Health and Disease, ed. Desmedt, J.E., New York: Raven Press, pages 213-226.

Kirkwood, P.A. & Sears, T.A., 1976 The average common excitation (ACE) potential and its significance. Journal of Physiology 259 pages 36-37P.

Kirkwood, P. A., and Sears, T. A., 1982 Excitatory post-synaptic potentials from single muscle spindle afferents in external intercostal motoneurons of the cat. Journal of Physiology 322 pages 287-314.

Kuno, K. and Miyahara, J.T., 1968 Factors responsible for multiple discharge of neurons in Clark's column. Journal of Neurophysiology 31 pages 624-638.

Landgren, S., Silfvenus, H. 1971 Nucleus Z, the medullary relay in the projection path to the cerebral cortex of group I muscle afferents from the Cat's hind limb. Journal Of Physiology. 218, pages 551-571.

Larrabee, M.G., 1958 Oxygen consumption of excised sympathetic ganglia at rest and in activity. Journal of Neurophysiology 2 pages 81-101.

Lee, H.C., and Milsum, J.H. 1971 Statistical analysis of multiunit multipath neural communication. Mathematical Biosciences 11 pages 173-180.

Martin, J.H. (1985) Receptor physiology and submodality coding in the somatic sensory system. Ch 23 In Principles of neural science, 2nd Edition. Kandel, E.R., and Schwartz, J.H., Publishers Elsevier Amsterdam. pages 287-300.

Matthews, P.B.C. (1966) The reflex excitation of the soleus muscle of the decerebrate cat caused by vibration applied to its tendon. Journal of Physiology 184 pages 450-478.

Matthews, P.B.C., 1972 Mammalian muscle receptors and their central actions. Edward Arnold Ltd London.

Matthews, P.B.C., and Stein, R.B., 1969 The regularity of primary and secondary muscle spindle afferent discharges. Journal of Physiology 202 pages 59-82.

McCandless, D.L., Zablocka-Esplin, B., and Espin, D.W., 1971 Rates of transmitter turnover in the cat superior cervical ganglion estimated by electrophysiological techniques. Journal of Neurophysiology. 34 pages 817-830.

Milgram, P and Inbar, G.F. (1976) Distortion suppression in neuromuscular information transmission due to interchannel dispersion in muscle spindle firing thresholds. IEEE Transactions on Biomedical Engineering BME 23 pages 1-15.

Moruzzi, G., and Magoun, H.W. 1949 Brainstem reticular formation and activation of the EEG. Electroencephalogr. Clin. Neurophysiol. 1 pages 455-473.

Poppele, R. E. & Terzuolo, C. A. 1968 Myotatic reflex: its input-output relation *Science* 159 pages 743-745.

Prochazka, A., 1989a Ensemble Inputs to α -motoneurons during movement. In "The Motor Unit: Physiology, Diseases, Regeneration." Ed. R. Dengler. (U&S: Munich) pages 32-42.

Prochazka, A., 1989b Sensorimotor gain control: A basic strategy of motor systems. Progress in Neurobiology 33 pages 281-307.

Prochazka, A., Hulliger, M., Zangger, P., and Appenteng K., 1985 'Fusimotor Set' : New evidence for an α -independent control of τ motoneurons during movement in the awake cat. Brain Research, 339 pages 136-140.

Prochazka, A., Hulliger, M., Trend, P. St.J. and Dürmüller 1988 Dynamic and static fusimotor set in various behavioural contexts. In Mechanoreceptors: Development, Structure and Function Eds. Hnik, P., and Soukup, T., Pergamon Press. London, pages 417-430.

Prochazka, A., Trend, P., Hulliger, M., and Vincent, S., 1989 Ensemble proprioceptive activity in the cat step cycle: Towards a representative look up chart. Progress in Brain Research 80 Eds: Allum, J.H.J and Hulliger, M., pages 61-74. Amsterdam: Elsevier

Redman, S., and Walmsley, B., 1981 The synaptic basis of the monosynaptic stretch reflex. T.I.N.S. 3 pages 248-251.

Ritchie, J.M., 1974 Energetic aspects of nerve conduction: The relationships between heat production, electrical activity and metabolism Progress in Biophysics and Molecular Biology 26 pages 149-187.

Roberts, W.J. Rosenthal, N.P. & Terzuolo, C.A. 1971 A control model of stretch reflex. Journal of Neurophysiology. 34 pages 620-634.

Rudomín, P., 1980 Information processing at synapses in the vertebrate spinal cord: Presynaptic control of Information transfer in monosynaptic Pathways. In Information processing in the nervous system. Ed Pinsker, H.M. and Willis W.D. Jr. Raven Press New York pages 125-155.

Schwindt, P.C. and Calvin, W.H., (1973) Equivalence of synaptic and injected current in determining the membrane potential trajectory during motoneuron rhythmic firing Brain Research 59 pages 389-394.

Shannon, C.,E., and Weaver, W., 1949 The Mathematical Theory of communication. University of Illinois Press.

Skok, V.I., 1973 Physiology of Autonomic Ganglia pages 139-53 Tokyo: Igaku Shoin.

Stein, R.B., 1967a Some Models of Neuronal Variability Biophysical Journal 7 pages 37-68

Stein, R.B., 1967b The information capacity of nerve cells using a frequency code. Biophysical Journal 7 pages 797-826

Stein, R.B., 1967c The frequency of nerve action potentials generated by applied currents. Proc. Roy. Soc. 167 Series B pages 64-86.

Stein, R.B., and Matthews, P.B.C. 1965 Differences in variability of discharge frequency between primary and secondary muscle spindle afferent endings of the cat Nature 208 pages 1217-1218

Stein, R.B., and French A.S., 1970 Models for the transmission of information by Nerve cells. In Excitatory Synaptic Mechanisms. (Proc. Of 5th Int. Meeting of Neurobiologists. Eds. P. Anderssen & J.K.S. Jansen pages 247-257

Stein, R.B. and Oğuztöreli, M.N. 1976 Does the velocity sensitivity of muscle spindles stabilize the stretch reflex? Biological Cybernetics, 23 pages 219-228

Terzuolo, C.A., 1970 Data transmission by Spike Trains. In The Neurosciences (a second study program) Ed. F.O. Schmitt. Rockefeller University press New York

Van der Kloot, W., 1977 Variables affecting electrical stimulation. In Functional Electrical Stimulation Eds Hambrecht, F.T. and Reswick, J.B., Published by M.Dekker N.Y. & Basel. pages 355-366

Walmsley, B. 1989 Synaptic potentials evoked in cat dorsal spinocerebellar tract neurones by impulses in single group I muscle afferents. Journal of Physiology 415 pages 423-431.

Wiley, R.G., Spencer, C., and Pysh, J.J., 1987 Time course and frequency dependence of synaptic vesicle depletion and recovery in electrically stimulated sympathetic ganglia. Journal of Neurocytology 16 pages 359-372.

Windhorst, U. (1988) How Brain-like is the Spinal Cord. Studies of Brain Function 15 Springer-Verlag.

Yamamoto, C., and Kurokawa, M., 1970 Synaptic potentials recorded in brain slices and their modification by changes in the level of tissue ATP. Experimental Brain Research 10 pages 159-170

Zablocka-Esplin, B., and Espin, D.W., 1971 Persistent changes in transmission in spinal monosynaptic pathway after prolonged tetanization. Journal of Neurophysiology. 34 pages 860-867.

APPENDIX

**MASSAVG DATA ACQUISITION AND
ANALYSIS PACKAGE FOR THE
CED 1401 AND IBM PC SYSTEM.**

Written By

Simon Connel (C.E.D.)

And

Steven Vincent (U. of Alberta)

MASSAVG DATA ACQUISITION AND ANALYSIS PACKAGE
FOR CTD 1401 AND IBM PC/AT SYSTEM.

Introduction	78
Loading and running the Program	78
The Main Menu	81
Setting up and Calibrations.	83
The Engineering Menu	83
Setup and Calibration	87
Assigning the Massram	89
Sampling Data	90
Replaying Data	90
Viewing Data	91
Data Inspection	92
Averaging	95
Averaging Set up	95
Averaging Screen	96
Filing Options	99
Parameter files and Display type selection	101
Pointer Manipulation Programs	103

	77
Special 1401 commands	104
Paintbrush and the MassAvg program	106
Index	109

Revision Date 10 October 1990

Introduction to the MassAvg Data Acquisition
and Averaging Package for the 1401.

This program uses the CED 1401 with a MassRam card (256Kb, 2Mb or 8Mb) to record analog (and digital) data on up to eight channels. It is designed to be highly interactive and most commands are based on single key strokes.

A maximum of 4 channels of the recorded data may subsequently be output through the 1401's DACs. Recorded data can be saved and restored on disks or displayed on the screen.

The **View** option allows the selection of data sections for analysis from large amounts of data by scanning a single channel.

Such sections can then be examined or compared in the **Inspect** option and pointers set for the averaging of segments of data. Also when calibrated, accurate measurements may be taken and the axis will be labelled accordingly.

Hard copy is available on Epson type dot matrix printers and HP digital plotters with provision for the printing of a title (limited to 80 characters) and labels for the Y axis.

Image export is provided in Zsoft Paintbrush and HPGL forms so that graphics manipulation programs may be used to enhance the final output and then combined with text using Desktop publishing software.

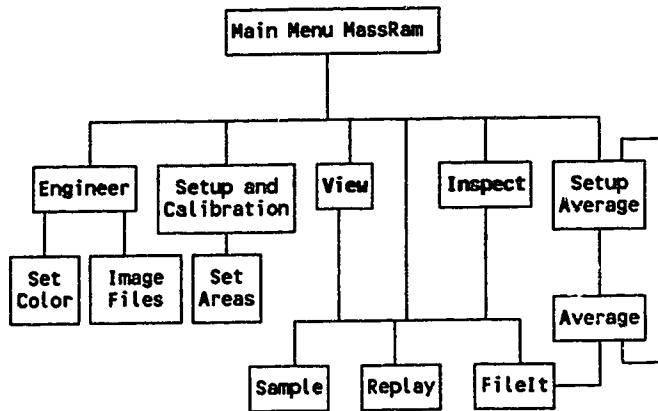
Short sections of data can be written out in ASCII form for analysis by other programs if needed.

Loading and running the Program.

First make sure the Metawndo driver is resident and then select an appropriate PrintScreen program and load this. (The MetaWindows printscrn utility is expected but others may be substituted. Then type

MASSAVG <filename> <display type>.

<filename> should be the name of the file in which to keep a record of the parameters used by you.
<display type> is the type and mode for the graphics card you are using, it need only be specified once, when the parameter file is first initialized. (A list of screen cards and modes supported will be displayed if none is specified or see the appendix on parameter files and display type selection below.)

Table I Overview of the MassAvg program.Input and Output.

Number of channels	Any selection of analog channels 0-7 Or two analog and one event input (Channel 8). (The D-15 ports 8-15 can be mapped as 0-7)
Input range	-5 to +5 (without optional gain/filter card)
Output Range	-5 to +5

General Information

There are several fundamental principles behind the operation of the program; These will be explained here before proceeding to the actual options available from the program.

The program supports 1401s with any size of MassRam (be it 256K bytes, 2M bytes or 8Mbytes). The MassRam may be divided into eight areas by the program. These may or may not overlap with each other and each is a multiple of 1K points long (2048 bytes) and starts after nK points into the MassRam (shifted by the number of channels so that precession of channels between areas does not occur). There is a concept of the "current area" which is the area to be sampled into, replayed, filed etc. Each area contains two entirely independent sections, one of which is the "current section" for that area. Where as the areas are defined in terms of memory usage, the sections are defined as an offset and duration in seconds from the start of the start of the area. Thus the amount of RAM occupied by a section is a factor of the sampling rate, duration and number of channels. Each area has a list of ADC/DAC channels and rates associated with it and each section carries independent parameters for displaying those channels. Within each section there is an active channel whose parameters can be changed.

Up to 100 pointers can be set, these point to a specific time offset into the current area and are used to generate averages. Both a duration and an relative offset being specified in the Average set up menu so that events before and after the mark can be examined in the average. Since the pointers are set by hand any consistent event in any channel (or channels) can be used without needing complicated logic or additional channels to identify and mark reliable triggers.

Tramlines are used extensively throughout the program. These consist of a thin line representing the maximum extent of the data with a thick section representing the visible section of the trace.

Entry of Text or Numerical Data.

Several of the options throughout the program require the entry of numerical or textual information. In all such cases the following rules apply:

- a) Input is done on the basis of changing the original text string. Thus a string is edited to achieve the required result, rather than re-keying everything from scratch.
- b) <ESC> clears the entry field enabling entry of totally new information.
- c) Both delete and Backspace keys are functional.
- d) <Home> moves the cursor to the start of the string.
- e) <END> moves the cursor to the end of the string.
- f) <TAB> moves the cursor to the first . in the string, normally the decimal point of numeric values.
- g) The left/right cursor keys move the cursor one character.
- h) <Enter> terminates entry of the string. If, at this stage, the field is empty then the string reverts to its original value.
- i) Any other key adds the corresponding character to the string until the maximum length is reached.

Hard Copy.

In several screens provision is made to produce hard copy of the current screen. Where this is possible there are normally three options:

- F3 Produces a simple screen dump to an Epson or IBM compatible printer via LPT1:. This requires that the Printscrn utility has been installed into memory. If you wish to use a different screendump utility you may but the program will not recognise it and so will produce a warning which can then be overridden if you are sure that you have a suitable program resident. The PRTSCRN utility will return control if the printer is not available but some alternatives do not (i.e. MS-DOS Graphics.Com). The program will provide a form feed at the end of each plot.

F4 This produces a drawing on a HP type plotter connected to COM1 using the parameters set in Engineering. This is based on recalculated values and so is at a much higher resolution than the screen. If the Baud rate is set to 'File' then the plot commands are redirected to a disk file that can be plotted later or used by other programs.

Shift F3 Invokes a routine that saves images as .PCX files for use by a batch printing program or editing by one of the Paintbrush programs from ZSoft. See Paintbrush and Massram in the appendix.

Before any of these procedure starts the Menu line at the bottom of the screen is overlaid with a title which may then be edited by the user.

The Main Menu

Select the required menu item with the function key or directly swap memory areas using the numbers.

Key **Function**

Analog Data Functions.

F1 Sample data into the current MassRam area (see Chapter 'Sampling Data').

F2 Replay data from the current MassRam area (see Chapter 'Replaying Data').


```

Mass RAM sampling package V1.00
Revision Date 29 July 1988
Author S. Connell & S. Vincent
Active Memory Area 1

1 2 3 4 5 6 7 8 9 10 11 12 13 14 15 16 17 18 19 20 21 22 23 24 25 26 27 28 29 30 31 32 33 34 35 36 37 38 39 40 41 42 43 44 45 46 47 48 49 50 51 52 53 54 55 56 57 58 59 60 61 62 63 64 65 66 67 68 69 70 71 72 73 74 75 76 77 78 79 80 81 82 83 84 85 86 87 88 89 90 91 92 93 94 95 96 97 98 99 100

1Sample 2Replay 3Envr 4Setup 5View 6Inspect7Average8. 9File 0Quit

```

Set Up Functions,

- F3 Set up various constants mostly affecting plotting functions (see Chapter Engine r).
- F4 Area setup and calibration functions (see Chapter 'Setup and Calibration ').

Data Display and Analysis

- F5 **View** (View one channel through the whole Massram
- F6 **Inspect**, allows the detailed examination of data in the selected memory area and the setting of markers for averaging. (see Chapter 'Inspect').
- F7 **Average**. This superimposes short sections of data from a series of preset key points and then produces simple mean averages. The digital information is converted to a Peri Stimulus Time Histogram. (see Chapter 'Averaging').
- F9 Main file handling menu also called from **Inspect** and **View**.
- F10 **Quit** (To DOS).
- 1-8 Select that memory area.

Setting up and Calibrations.

The program is initially configured using two main menu options, Engineering and Setup.

The Engineering Menu

This menu is used to set values that are normally constant on any one machine or only rarely changed by the user. These include the parameters of the serial port for the plotter or the maximum number of points to display at a time.

The item to change is selected using the up/down cursor keys. When the required item is highlighted the <RETURN> key is pressed and the required value is entered in the usual way. Note that some items merely toggle around the legal values with each <RETURN>.

The required option is selected by use of the up and down arrows to reach the line and then pressing <RETURN>.

Single Channel maximum rate

(Multiple channel maximum if Z8 installed).

This is the maximum sample rate (Using ADCMR,F or ADCMEMF) which can be achieved with a single channel (the aggregated rate using multiple channels with a Z8 equipped 1401). This should be 82500 for a 5000 series 1401 with standard ADC 66666, for a pre 5000 series 1401)

Multi channel (without Z8) max rate.

The maximum aggregate sampling rate without the Z8 if using multiple channels. Usually 42000 for a pre 5000 series 1401.

Maximum interrupt driven sampling frequency.

The maximum interrupt driven sampling rate to use. There is an advantage to using interrupt driven code as this allows us to display data as it is acquired. We suggest a maximum 15000 for pre 5000 series units and 30000 for the post 5000 series. This sets the boundary between 'fast' (only a progress box on screen) and 'slow' (with channel monitor) sampling.

Example Samples are interrupt driven if longer than

The setup option maintains a display of the current channel sampled at a current rate for the area. If this rate is low it could take a long time to fill the sample buffer and the program would feel sluggish. Use this parameter to set the longest period between screen updates. This will force the use of interrupt driven sampling, where possible. Half a second is reasonable for most users.

Number of points per line in Inspect.

In **Inspect** there is a maximum number of points which can be displayed per trace (16000). Since the more points that need to be drawn the longer each screen update takes, we suggest this value is kept fairly low. 2000 is reasonable for most applications. This value also affects the number of points sent to the plotter and may limit the length of any average, since every point is used to generate the average.

Number of points displayed while sampling (or in view).

This sets the points per line for **View** as the proceeding option does for **inspect**. This is also the number of points displayed in the setup option or during the slow sampling modes where a display is maintained.

Displaying ALL points while sampling.

If **TRUE** then the display is updated as often as possible, giving the effect of a stream of data scrolling in from the right (beware that with some speeds the display can get significantly behind the actual sampling). If **FALSE** then the display is of a specified length of time and the display does not scroll. Instead, the display window fills from left to right and when full clears out and starts again. Note that in this mode not all points are displayed, unless the sampling rate and time per screen are very low but screen response is fairly well instantaneous.

If FALSE display screenfuls of

The time per screenful of data to display when sampling at "slow" rates (where a display is maintained) and the above item is set **FALSE**.

Offset increment in Inspect

The fraction of a screenful to move the trace when inspecting data. This applies to the x axis using **CTRL PgUp/Dn** or the Y axis using **Home/END**.

Zoom Multiplier in Inspect

The fraction of a screenful to zoom in or out. The smaller the number the greater the change. This applies to the x axis using PgUp/Dn or to the y axis using the up or down arrow keys.

Select inputs

The 8 analog channels used by the program can be switched between the 8 BNC sockets (normally channels 0-7) or the D-15 socket (normally 8-15). The program treats the 8-15 channels internally as 0 - 7 and the two sources cannot be mixed. The D-15 is sometimes more convenient when connecting to standard setup.

Left hand side of plotter box

Right hand side of plotter box

Bottom of plotter box

Top of plotter box

These are used if a HP plotter is connected to define the plot window in absolute plotter units. The values 1000,10000,100,7000 will produce a sensible plot on most HP plotters (and compatibles).

Baud rate for the serial line to the plotter

Parity for the serial line to the plotter

Stop bits for the serial line to the plotter

Data bits for the serial line to the plotter

These four parameters set up COM1 to communicate with a plotter. We suggest that you set the highest baud rate possible but these values must agree with your plotter settings. Baud rate may also be set to 'File' this then uses the same directory and root file name plus a number to create a series of plot files that can then be sent to a plotter in batch mode or imported into other programs.

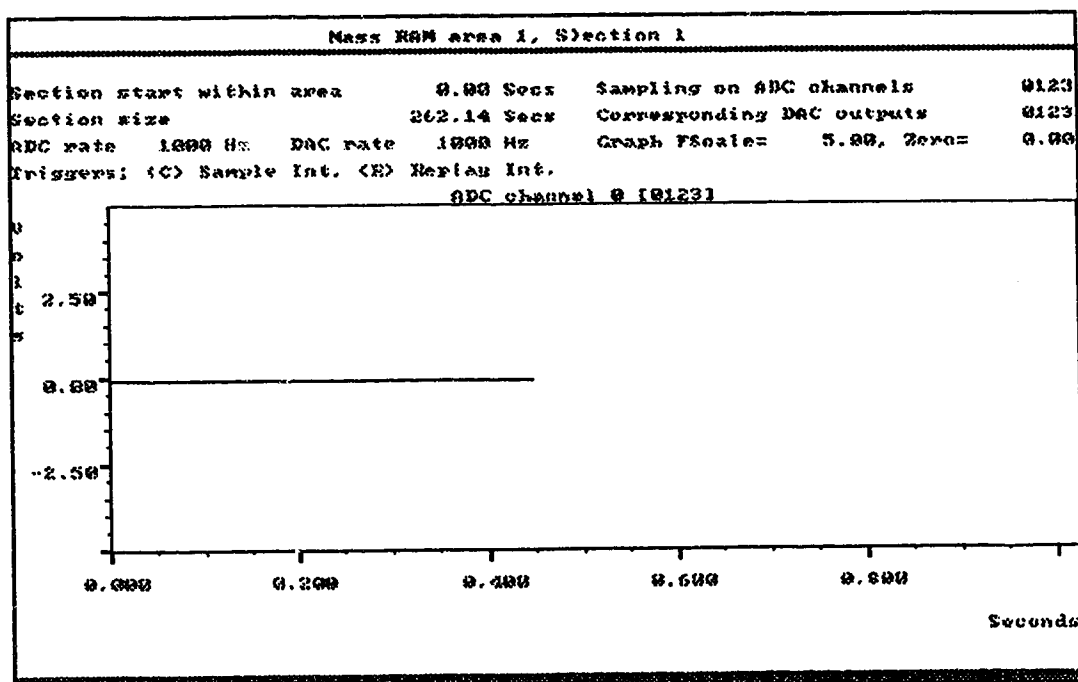
Function Keys.

- F3 Colours setting mode. This enables the user to change the colours used by the program. To do this the user moves to the relevant line and presses <RETURN> until the desired colour shows on the right.
- F4 This brings up the same menu as saving an image to disk and enables the user to specify the root file name and directory to be used for export files such as .PCX (ZSoft paintbrush) .PLT (HPGL) and .LST (ASCII) files. These file specifications are combined with a number to form a continuous series of files. This is so that the user can then use other (batch) printing programs (such as LaserPlotter by Insight Development) to produce hard copy but they also provide a useful export function for use with Desk-Top Publishing programs.
- F10 Quit to main menu.

Setup and Calibration

The setup menu is called from the main menu by pressing function key 4.

This part of the program is used to divide the MassRam into independent areas, each with its own set of analog input channels, analog output channels, calibrations, sampling and replay rates. All the options defined here are remembered in the parameter files, so most users will only need to set this once. Since memory areas may overlap it is often useful to assign different tasks to different areas even though they overlap.



A constant display of the current channel for the current section of the current area (the current channel for short) is maintained in the display window. This feature is available so that a signal may be checked before actually sampling it into the MassRam. It is recommended that the signal should fill as much as the $\pm 5V$ range as possible so that the most is made of the 1401's 12 bit resolution.

KEY Operation

- 0-7 Changes the current channel (and hence the display) to the channel specified.
- 8 If the special digital channel is used then change this channel to set the axis but no display will be maintained. Actually the event 0 input.

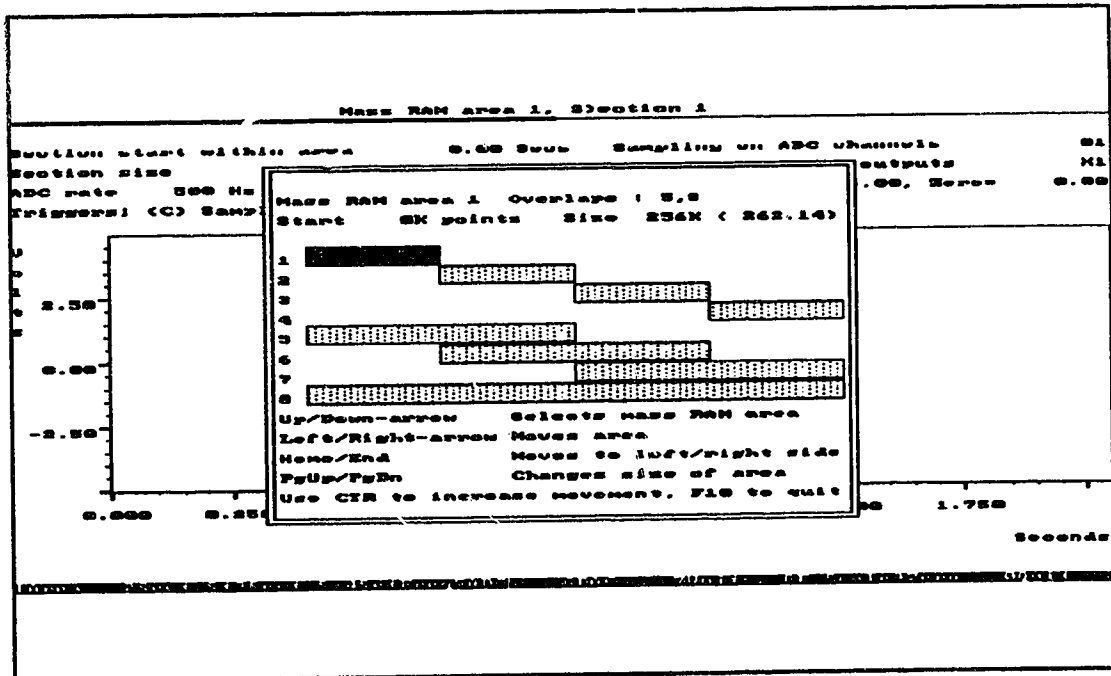
- S Toggles between the two sections of the current area (and hence the section to be setup). Note that toggling the section will leave sampling rates and channel lists the same but may change the active channel or the levels of zooming.
- C Toggles the sample mode between auto trigger (C) and external trigger (CT) modes. For Sampling the external trigger should be a low going pulse on event 4 input.
- R Toggles the replay mode between auto trigger (C) and external trigger (CT) modes. For Replaying the external trigger should be a low going pulse on event 3 input.
(Note the 1401 technical manual explains how to change this to high going if that is more convenient)
- F1 This is used to divide the Massram between the different memory areas. See Assigning the MassRam below.
- F2 Set the start of the current section. This is entered as an offset in seconds from the start of the area. This has the same effect as setting the start cursor in **View** or specifying an **O**ffset in **I**nspect.
- F3 Set section length. This is also in seconds and can also be set using the cursers in **View** or **D**uration in **I**nspect.
- F4 Set Rates. The sampling rate and replay rates are entered here. The program will then find the nearest possible rate using the available clock/counters to drive the ADC and DAC channels. There are two separate rates to allow data to be replayed out slower or faster than the sampling rate. This might be wanted to match the signal speed to that of a chart recorder or scope.
- F5 Select the ADC Channels. This is done by editing the existing list. The only restriction on order is that channel 8 if used must be the last of three channels used and no channel may be specified twice.
- F6 Select the DAC channels. This is the list of DACs on which to replay previously sampled data. Dummy channels (X) are used to skip unwanted channels so that any combination out of the eight, can be replayed through any of the 4 DACs but no output may be specified more than once. If the ADC channels are edited this string will also be adjusted to maintain any existing correspondence.
- F7 Specify the units for the y axis. This is a title used for the Y axis which appears on the screen and plotter output. A different value may be specified for each channel.
- F8 Set full scale reading. This provides a scaler for the current channel. For instance if the units are "Volts" then a full scale value is 5 but if mV are used then the full scale is 5000. This value can be used to compensate for any pre-amplification stages used so that the y-axis units and the values of the cursor read out are in meaningful units.
- F9 Change the value corresponding to a grounded ADC input. This is useful if a DC offset has been added to a signal so that the full +/- 5V ADC range could be used by a signal that was not evenly distributed about ground. i.e. a rectified e.m.g.
- F10 Quit. Returns control to the main menu.

Assigning the Massram

Called by pressing F1 inset up above this option is for tailoring the use of the MassRam by the eight areas. A pictorial representation of these areas in the MassRam is given with the current area highlighted. The display at the top tells you which channels overlap the current area, its start and size in k points and its approximate size in seconds. The independence of areas and sections means that up to 16 different sections can be set for replaying out of the DACs to drive experiments or several different 'views' of the same data arranged for comparison. It is also recommended that each individual task be set up in its own area so that the parameters are kept constant.

Up/Down arrow Selects the MassRam area.
 Home/End Moves the area to the left or right ends respectively.
 Lft/Right Moves the area. Use of Control speeds up this movement.
 PgUp/PgDn Changes size of the area. Control changes rates of growth.
 F10 Quits.

NB. Care is taken that each area starts at a point that is an integer number of channels from 0 so that channel wrap-round is prevented.



Sampling Data

Sampling is possible from the main menu and **Inspect** or **View**. From the main menu the sampling proceeds until the whole area is filled, by comparison Sampling initiated from **Inspect** or **View** only fills the current section of the area. In both cases this is started by pressing function 'key 1 and sampling will not start until a 'Y' is pressed to confirm. This is to prevent accidental sampling over data and also reduces the delay between signalling the desire to start sampling and the first sample. Sampling and may be stopped at any time by pressing 'A' (abort).

If the sampling is at a high rate ("fast"), then a message will be displayed indicating the progress as a percentage completed. If possible, when the sampling rate is low enough a display of one channel of data will be maintained on the screen. This may be in one of two ways, as determined in Engineer above.

- a) Every point is displayed and the display is updated repeatedly, giving the effect of data scrolling from right to left across the screen. Only really practical on fast machines with very fast displays.
- b) Data sections of a pre-specified length are displayed sequentially until the sampling is finished.

In both cases a Tramline at the bottom shows the progress of the sampling. In both display methods the channel displayed may be changed by pressing the number of the desired channel at any time.

Replaying Data

Replay is very similar to Sampling above but has no display option, a percentage of completion being shown instead. This option is activated by pressing F2 on the Main menu, **Inspect** or **View**. Like sampling above the whole area is played out from the main menu compared to the section only from **Inspect** or **View**. This can be useful if you only wish to reproduce short sections, either to drive a muscle puller other equipment. The digital outputs are used to provide a trigger signal, going high while the signal is replayed.

Since the replay rate can be different from the sampling rate fast signals can be sent slowly to a chart recorder with limited bandwidth or large amounts of slowly sampled data can be sent quickly to a scope.

As in sample above pressing A will abort the sending of data and return you to the calling menu.

A cyclic replaying of the section can be initiated by using Ctrl-F2 from **Inspect** or **View**. No percentage display is maintained and A(bort) then stops the output at the end of the cycle. The digital output lines will go low between each repetition of the section.

Viewing Data

The **View** option is used to display a single channel of an entire area and also to modify the section boundaries for use with the **Inspect** option. The data is displayed as six traces across the screen.

A pair of solid cursers mark the start and end of the current section within the area. A dotted cursor can be moved round the screen and used to set the boundaries of the current section or pointers for averaging. It is possible to change sections or channel with corresponding changes shown on screen.

Since it is generally too slow to draw every point in the area every nth point is shown. The interleave factor used is shown in the top left of the screen. The total number of points drawn can be set in "Engineer" to provide the best compromise of speed and resolution.

This option allows the sampling, replaying or filing of sections as well as the whole area without returning to the Main menu.

Hard copy may be produced on Epson or IBM compatible printer or a HP style plotter.

Key Operation

- O-8 Changes the current channel (and Hence the display) to the channel specified. (If active).
- S Swap to the other section.
- F1 Sample data into current section (see Sampling).
- F2 Replay Section (see Replaying).
- F3 Produce Hard copy onto an Epsom printer.
- Shift-F3 saves the image to disk in .PCX form.
- F4 Produce Output on HP plotter.
- F5 No function.
- F6 Choose. Sets a pointer for the averaging option.
- F7 Sets the start of the current section to the position of the dotted cursor.
- F8 Sets the end of the current section to the current cursor position.
- F9 Activates the filing menu.
- F10 Quit.

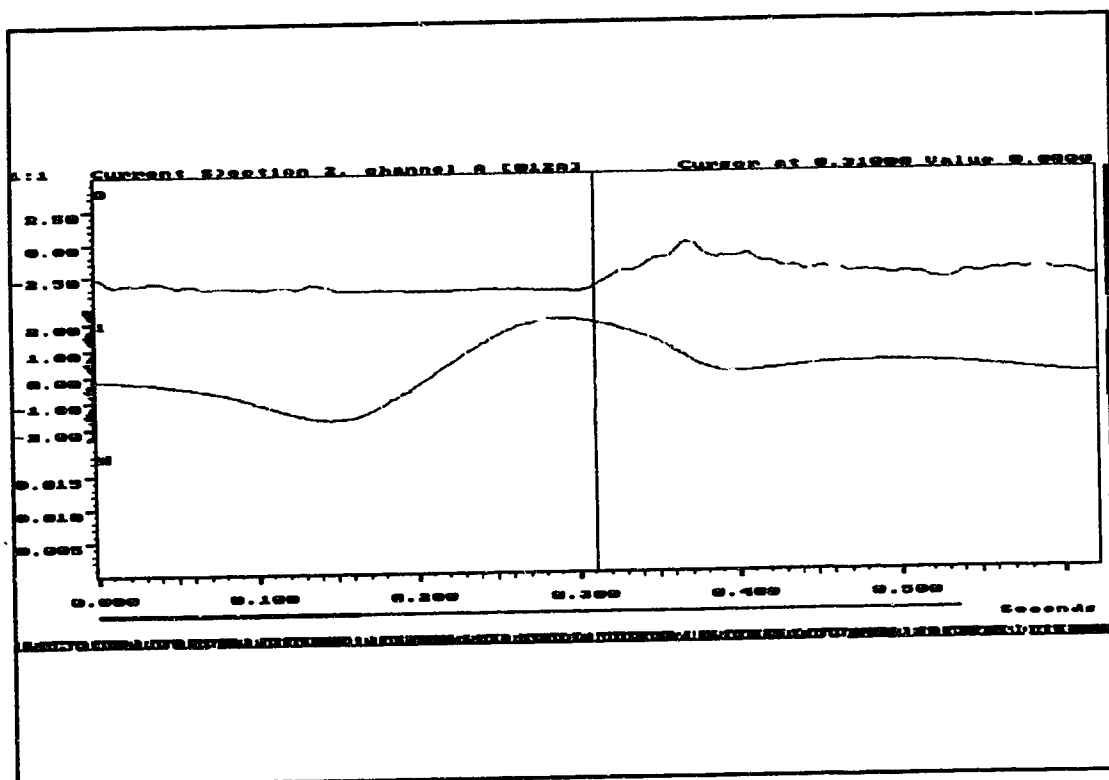
Cursor Keys.

- Left Move cursor left. Control speeds this up.
- Right Move cursor right. Control speeds this up.

Up Move cursor Up.
Down Move cursor Down.

Data Inspection

Selected from the main menu by pressing function key 6, this option allows cursor analysis of previously sampled data. Similar to **View**, **Inspect** allows sampling, replaying and filing of data within sections and without returning to the main menu. From this display you can also set a series of "trigger" points which then will be used to submit short sections of data for averaging.



The basic display is a trace showing the current channel from start to end of the current section. More complex options allow all the channels to be inspected and both sections to be displayed at once.

At the top of each section display is a line of text giving the current section, the channels in use and stating the position of the cursor relative to a moveable baseline and the value of the current channel at that point. This is in the Units defined for that channel.

Below and to the right of each section are "tramlines" which indicate the amount of zooming which has been done in the x and y directions respectively.

At the top left of each section is the interleave factor used by the display. e.g. 1:16 means that only every sixteenth point from the MassRam is actually being displayed. With instantaneous frequency displays this is important because at values other than 1:1 events may be missed.

Key assignments for INSPECT

- F1 Sample data in current section (see Sampling).
- F2 Replay Section (see Replaying).
- F3 Produce Hard copy onto an Epsom printer.
- Shift-F3 Saves the image to disk in .PCX form.
- F4 Produce output on HP plotter or in a .PLT file.
- F5 Sets/releases a base line at the current cursor position so that the time read off by the cursor is relative to this point or the start of the area.
- F6 The current cursor position is recorded for use in averaging.
- F7 Toggles the number of viewing sections shown on screen at one time (one or two).
- F8 Copies the parameters of the current section into the other one.
- F9 Calls the File menu.
- F10 Returns to the main-menu.
- Del Clears the buffer of selected pointers.
- H Help. Brings up a short reminder screen on the actions of the alpha keys not shown on screen. As detailed below.

Channel Controls

0-8	Choose active channel. (Note 8 is the digital/pulse frequency channel)
Down Arrow	Zoom Out on active channel.
Up Arrow	Zoom in on active channel The amount of zoom is set in the Engineering option.
I	Invert the active channel. (Channel label becomes marked with a -)
M	Magnify. The Y scaler becomes the value specified.
V	Vertical Shift (-ve Up +ve Down!)
W	Writes the active channel on screen into an ASCII file. This file contains the channel number and the value in seconds of the left hand margin on the first line and then the raw values of each point on screen for that channel.
Home	Move active channel up the screen.
End	Move active channel down the screen.

Section Controls

A	Switch display between active channel only and all channels.
C	Combines 'D' and 'O' below.
D	Sets the duration (in seconds displayed).
L	Left. Sets the offset (Left margin) to the cursor position.
O	Sets the starting position of the displayed section.
S	Toggle between viewing sections.
PgUp	Increases the time displayed.
PgDn	Decreases the Time displayed. (as set in Engineering).
Ctrl PgUp	Move viewed section right through Massram.
Ctrl PgDn	Move viewed section left through Massram.
Ctrl Home	Resets everything to defaults.
Ctrl End	Forces a screen redraw.

Cursor controls.

The left and right arrows move the cursor right and left respectively. The control key speeds up this movement and when the cursor reaches the edge of the screen it is redrawn with the cursor moved to the middle.

Averaging

This option can be selected by using function key 7 from the main menu once some pointers have been selected. (You may use a previously saved pointer file.) This option first calls the averaging setup menu (Below) and then enables the build up of complex displays showing each selected section overlaid.

Averaging Set up Menu.

When averaging is selected from the main menu this menu appeared immediately. This enables the user to select the durations and offsets of the average generated and to specify the name of the file in which the pointers may be saved or loaded from.

```

MassAvg Averaging package V1.1f

Data Filed in                .Thisfile
Pointer file                 Pointers
Length of average           5.0000
Start Offset (from Cursor)  -2.0000
Bin Width for Pulse frequenou  10.
F9 File Menu F10 Proceed
  
```

This menu has 5 lines.

- Line 1 Space is reserved here for the name of the data file the pointers in use should be associated with. If used it will allow the user to identify the correct data to go with a selected pointer file.
- Line 2 This line is where the name of the pointer file is specified, this is used for filing or loading pointer files.

- Line 3 Enter here the time in seconds over which to average. At present this is limited to about one third of the space available to the 1401s 6502 processor since a double precision running total is kept until the user asks for the average.
- Line 4 This enables the specification of an offset from the pointer value at which to start the average. (- before + after).
- Line 5 Bin Width. This sets the width as a number of samples used to average the digital channel (8). This is used to create a bin histogram of events on channel 8.

F9 Pressing this key will bring up a short filing menu

S Save Pointers in the file specified.

L Load Pointers from the file specified.

P Print Pointers. This prints a short report on the printer that specifies the pointers selected, the channels in use and the sampling rate.

At present it is not possible to change directory from this menu, all filing operation will be carried out in the previously selected directory.

F10 This quits the Averaging setup menu and returns you to the averaging section proper.

F10 Quits back to the above menu.

Averaging Screen

This option steps through a series of sections of data superimposing each in turn and then produces an average of those sections on the screen. The alignment of different sections can be improved using the Nudge keys and inappropriate selections may be deleted. If a colour screen is used then the most recent plot is shown in a different colour so that it can be distinguished more easily.

The top left of the screen tells you which is the most recent segment and the total number of segments available. When an average is produced this message changes to tell you how many segments were averaged and the total number of segments.

F1 Brings up the Averaging Set up Menu so that any parameters may be changed.

F3 Invokes the printscreen function allowing the specification of a title on the bottom line.

Shif F3 Creates a .PCX image file as in *Inspect*.

F4 As above but sends the information via the serial port to a plotter or a disk file. (Note raster plots can generate very large plot files, make sure that your hard disk has enough space.)

F5 Clears the screen and the averaging buffers so that a new average may be started.

- F6** Calculates and plots the average on screen. Initially drawing the average over the superimposed plots, Then on pressing **F5** or **F10** will clear the screen and draw the average on its own. Note the average is produced from those segments actually on screen but this may be any continuous series from the pointer list. A further **F5** or **F10** is needed to return to the raster generation. The final average is left on screen so that it may be combined with a couple of typical segments afterwards.
- F7** Step; this is used to step through the selected data sections one at a time, each press invokes **F5** and then draws the next section.
- F8** Build; This redraws any previous trace in to a background colour and then draws on the next section.
- F9** After **F6** above invokes the file menu to allow the filing of the generated average. The section flag is set to **AVG ('4')** and the default file type is **.MSA** while the average is available but if this is changed a new average will have to be generated for filing. A saved average may be reloaded and treated as data for replaying or comparison with other averages.
- F10** Quit to Main Menu.
- Del** This deletes an entry from the current pointer list and from the screen.

Channel Controls

- 0-8** Choose active channel. (Note **8** is the digital/pulse frequency channel).
- I** Invert the active channel. (Channel label becomes marked with a -)
- M** Magnify. The Y scaler becomes the value specified.
- V** Vertical Shift (-ve Up +ve Down).

Down Arrow Zoom Out on active channel.

Up Arrow Zoom In on active channel.

The amount is set in the Engineering option.

Home Move the active channel up the screen.

End Move active channel down the screen.

Cursor controls.

The left and right arrows move the cursor right and left respectively. The control key speeds up this movement.

Nudge Keys. ,<>.

The most recent section displayed can be moved laterally to improve its alignment if necessary using the keys marked < or >, this movement is fine if the keys are shifted and coarse if not (.). This adjusts the value held in the pointer list in memory and so is permanent. The pointer files on disk are not affected and can be used to restore the original list if mistakes are made.

Filing Options

Selected from the main menu, **View**, **Inspect** or **Average** by pressing function key 9. The filer allows several file manipulations to be performed as well as simple saving or loading of data.

There are four ways a file may be saved and each produces a file that may be freely loaded in any of the other ways.

- a) An entire area may be saved or loaded. When loading, the channel lists, zoom factors, sampling rates and section definitions are all restored, leaving all as it was prior to saving. This mode is the default from the main menu.
- b) Data in a single section is saved or loaded. When loading, the number of channels must be compatible with the existing area. None of the area definitions are changed and data is merely copied into the MassRam. If the file is longer than the section, then the data is truncated to fit. This mode of filing is the default when called from **Inspect** or **View**.
- c) Data between the base marker and the cursor in the current section is saved. Data is loaded directly after the cursor but is truncated if necessary to prevent it going over the end of the area. Otherwise as b) above.
- d) When an average is on screen (marked as section 4) it is possible to save the average alone. This is a special case of b) above.

The program uses the standard DOS conventions for wild card searches and directory structures. It is therefore recommended that the user be familiar with these and directory structures on a hard disk be explained by a local expert. (See also Appendix D.)

The Massram program creates 4 internal and 3 export file types distinguished by their type ending;

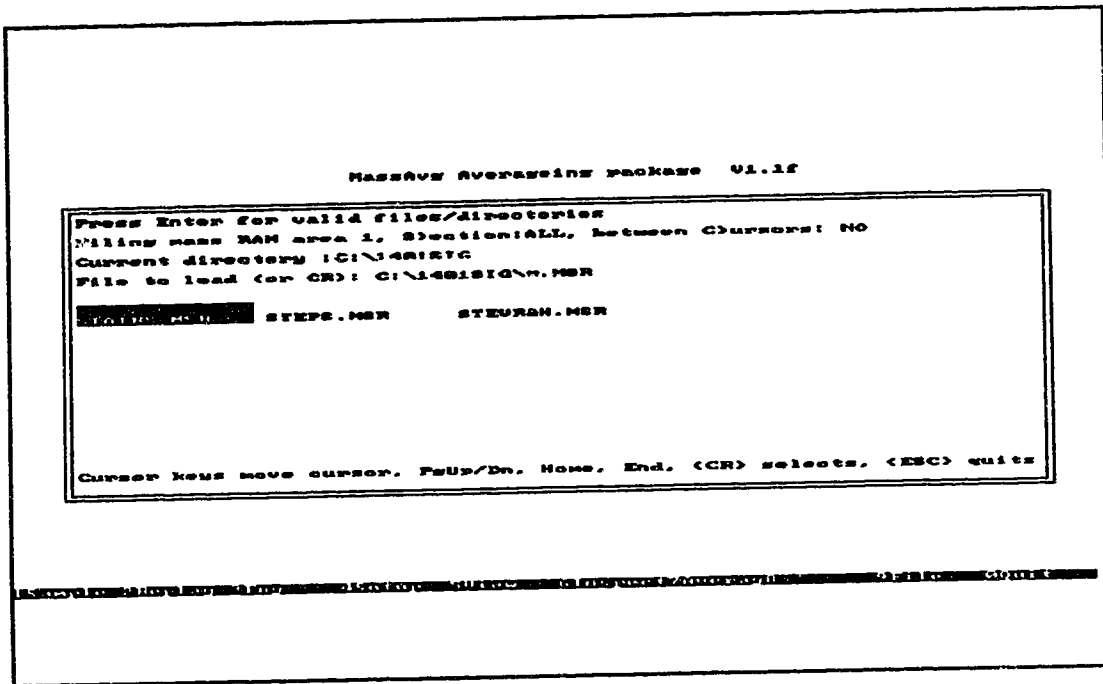
Internal

- .MR** Parameter files used to restore parameters when the program starts.
- .MSR** Data files containing actual data and a 1k header.
- .MSA** Data files containing an average that may be loaded as data.
- .MRP** Pointer files containing the offsets used to generate an average or raster.

Export

- .LST** An ASCII list of values for export to another program.
- .PCX** Image files for PC (or Publishers) Paintbrush.
- .PLT** Hewlett Packard graphics language (HPGL) plot files for HP compatible plotters.

The export files are named automatically in an ascending series for easy batch processing later. The directory and root name for these series is set from the engineer menu rather than from the filing menu.



Key Operation.

- S Toggle between filing section 1, section 2 or the whole area.
- C If a single section is being filed then this toggles between filing the whole section or just between the cursors. (Problems have been encountered with this !).
- F1 Gives a directory listing of the logged directory. Selecting a directory gives a listing of that directory. Press <ESC> to return to the main file menu.
- F2 Copies a file. The source name can be specified by typing it in or by using the interactive directory listing to select a file name. The destination name must be typed in.
- F3 Erases a file. Once the file has been selected the user must confirm the operation before the file is actually deleted.
- F4 Rename file. As with copy file this requires the user to select the file by using the directory or type the name directly. The new name must be typed.
- F5 Loads a file.
- F6 Saves a section or area into a file. Confirmation is needed if a file is going to be overwritten. Automatically adds type ending as appropriate.
- F7 Makes a new directory with the path specified.

- F8 Removes an empty directory. This can not be the logged directory.
- F9 Changes the current drive/directory.
- F10 Quits the filer.

When performing operations with files the selected file name may be typed in to the space or, if its name is not known, may be selected from a list of possibles on the disk. This is done by pressing <Enter> in response to the prompt for a filename. A list of files for selection then appears on the screen (all files in the current directory are listed unless a file is to be loaded in which case only files with the extension .MSR are listed by default). The usual DOS style wild cards may be used to narrow down the number of alternatives. Directories are shown in italics and selecting a directory causes that directory listing to be listed on the screen for selection. The first entry of a directory is always "." which indicates the parent directory.

The arrow keys move the cursor (inverse video) around the screen list.

PgUp/PgDn move between pages of the directory if necessary and <Home> and <end> move the cursor to the beginning or end of the list respectively.

Parameter files and Display type selection

Before invoking the MassAvg program, the graphics driver and any screen dump utility must be installed. To do this manually type the following;

- C>METAWNDO To load the graphics driver.
- C>PRTSCRN To load the Metawindow printscreen utility.

Alternatively these commands can be included in your AUTOEXEC file. If you use Sidekick it is recommended that MetaWndo is installed first. Since Sidekick only knows about standard IBM CGA screen modes I do not recommend its use when other graphics display modes are used. And since MassRam needs a lot of memory I recommend that you uninstall SideKick.

The MASSAVG program is invoked by typing MASSAVG followed by a series of optional command line parameters. i.e.

MASSAVG [<filename>] [<Display>] [M]

The simplest of the three is the last one which if present indicates that all screen output is to be in monochrome. This is only necessary when a monochrome monitor is used with a colour graphics card. It is not necessary to use "M" when a monochrome card is used.

<Display> is the video card mode and it specifies the type of graphics card and the mode to be used by the program.

<filename> The root name of the file (.MR) to hold the engineering and setup parameters. The two parameters above are also set from the values stored in this file unless overridden. If no filename is given then the program searches for the file DEFAULT.MR and uses that as its parameter file. If the file does not exist and no Display was given then the program will stop with an error, listing available graphics boards, one of which needs to be specified.

The file DEFAULT.MR is special because it is searched for automatically if no file is specified. It can be set up by specifying it when the program is first run.

The other parameters stored in these files include:

Graphics card type and mode.

Engineering values (including colours).

Calibration parameters.

Area mapping.

And for each area;

 Sampling channels and parameters.

 Replay channels and parameters.

 Inspect section parameters such as Zoom and Magnify.

Names other than DEFAULT may be used to define different parameter sets which will be used when specified in the command line. This is useful if the program is to be used for several different tasks or by different users. The first 5 characters of this name are combined with a number to create names for plot (.PLT) and image (.PCX) files.

Valid Screen Types

Colour;

DEB640X200	Olivetti or ATT 16 colour board.
DEB640X400	" " " " " "
CON512X512	Conographics cono-colour 40 adaptor.
CON640X400	" " " " " "
EGA640x200	IBM Enhanced graphics card and clones.
EGA640X350	" " " " " "
EVR640X200	

EVR640X400
 SIG640x400
 STB640X400
 TEC640X200
 TEC640X400
 TTS360X350
 NNR512X512
 VGA640X480

Number Nine revolution card (256 colour).
 VEGA Deluxe card and Multi mode monitor.

Monochrome

ATT640X400
 CGA640X200
 EGAMONO
 HER720X348
 MDS728X1008
 STB640X352
 STB640X400
 TEC720X352
 TEC720X704
 TTS720X350
 WYS1280X400
 WYS1280X800

Enhancement on CGA for Olivetti or ATT computers.
 Standard IBM and clone card
 Enhanced graphics monochrome mode.
 Standard Hercules or clones.
 MDS Genius Adaptor.

 Tecmar Graphics Master card.
 " " " "
 IBM PC-3270 Monochrome mode.
 Wyse WY-700 display.
 " " "

The serial line parameters may be varied interactively in the Engineering menu. If the parameter file is specified (see above) these will be read from it. This program runs the plotter in the hardwired handshake mode, using pin 20 on the plotter as the hardware restraint.

Pointer Manipulation Programs

The following utility programs have been written to generate pointer files for use with the MassAvg program.

CombPTR This takes two existing pointer files and combines them. It is useful if you wish to produce a grand Average display from several pointer groups.

AutoPoint This will produce a series of evenly spaced pointers from a single given starting point and increment.

ManPoint Produces a series of pointers by manual entry of the offsets in seconds.

Special 1401 commands**ADEVMR;**

This additional 1401 command was written for Dr. A. Prochazka at St. Thomas's Hospital London and is used to sample two ADC channels and one event channel (Event input 0, called channel 8 in the program above for convenience). For every clock tick the command stores the value on the two ADC channels and interrogates the event input. If a pulse has occurred then the time in 10 microsecond units is stored in the MassRam otherwise 8000 hex is stored as a null value if no event has occurred. This program allows the logging of a neurogram along with two related variables. Care is taken that 8000 h does not otherwise occur but no precautions are taken against to very close events (one is lost) or event clock overflow. This last can easily be detected afterwards.

ADEVMR,G,bank,st,banks,sz,ch0,ch1,clock,pre,count;

<bank> The 64k bank in the 1401 at which to start.
 <st> The offset in <bank> at which to start.
 <banks> The number of 64k banks to fill.
 <sz> The distance (in bytes) to sample above <banks>*64k.
 <ch0> The first analog channel.
 <ch1> The second analog channel.
 <clock> Trigger mode; C to select internal clock
 CT for triggered clock.
 F for the external clock.
 <pre> The first pre-scaler.
 <count> The second clock scaler.

ADEVMR,K; Abort sampling and re-initialize the command.

ADEVMR,?; state,bank,offset

Returns the sampling state and the address of the next byte to be written.

<state> May be;
 -128 = waiting for trigger.
 1 = Running.
 0 = Finished without error.
 -1 = Finished but ADC overrun error.

<bank> Bank into which the next byte of data will be written.

<offset> Offset in bank at which the data will be written.

KILL ;

Produced at the first CED user meeting as a simple way to remove down loaded commands without affecting data in the MassRam or processor memory. This command is useful to free processor memory in cases where there are a lot of down loaded commands used to collect data and then post sampling processing is to be done in the 1401.

MRHOST;

This command transfers up to 64k bytes at a time, from the host to the mass memory or the mass memory to the host. It can be used when one, but not both of ADCMR and MRDAC are running. The general form is:

MRHOST,dir,bank,st,hsz,adr[,skip[,byte]]

MRHOST,?; banks<CR>

<dir> Is R for read Massram, W for Write to it.

<bank> The 64k bank in the 1401 at which to start.

<st> The offset in <bank> at which to start.

<hsz> Is the size of data in bytes that the host will send/receive.

<adr> The absolute start address of the data area of the host.

<skip> Is the number of data points to skip over in the massram between reading/writing each point (use this for transferring interleaved data). Skip defaults to 0. Note that skip is in points rather than bytes so with 16 bit data skip*2 bytes will be jumped over in the massram.

<byte> Is set to 1 for eight bit data points or 2 for 16 bit data. The default is 2.

<banks> The number of 64k banks in the MassRam in the 1401. Use this to check for size before large transfers.

The timings for transfers are as follows:

Writing to MassRam

| byte | skip | rate /K Hz. |
|------|------|-------------|
| 1 | 0 | 100 |
| 2 | 0 | 113 |
| 1 | >0 | 28 |
| 2 | >0 | 46 |

Reading from MassRam

| byte | skip | rate /K Hz. |
|------|-------------|---------------|
| 1 | 0 | 100 |
| 2 | 0 | 111 |
| 1 | n (1 to 15) | $500/(5.5+n)$ |
| 2 | n (1 to 7) | $500/(5+n)$ |
| 1 | >15 | 25 |
| 2 | > 7 | 40 |

Paintbrush and the MassAvg program.

To transfer screens to Paintbrush it is not necessary or even desirable to use FRIEZE in place of the usual printscreen utilities. CTRL-F3 will invoke a separate overlay routine that will save the screen image in .PCX form. This routine has been tested on DEB640x400, EGA640x350 and VGA640x480.

The Overlay initially puts up a menu which enables you to change the default directory and file name root (the first 5 letters of the parameter file specified at run time). It also shows a number, this will form part of the file name so as to form a continuous series. The purpose of the number is to enable the user to create a continuous series of 'plots' for later printing. Plotting to a file uses the same directory and root but with a separate number and .PLT endings so that batch plots can be produced.

Some problems have been found with some monochrome modes so frieze or Pizzaz Plus can be used if for some reason the .PCX save does not work correctly.

For normal work there are two commands sequences, 1 to Print the screen and 2 to save the screen to disk.

1 TO PRINT

Press f3 and set the title.

Check that the printer is on.

Press the space bar.

Garbage should appear on the screen.

Type the sequence PN<Enter> The garbage will change with each letter.

After the <Enter> the garbage should disappear and the printer should start.

2 TO SAVE THE SCREEN TO DISK.

Press f3 (Print) and set the title.

Press the space bar.

Garbage should appear on the screen.

Press S for save.

Then type in a file name for the picture. If you are working on my machine I would suggest that you put a blank floppy disk in drive B and use names with the form B:<name>.PCX.

The garbage will disappear and the relevant disk drive light should come on.

The format .PCC is the form used by Paintbrush to indicate a cutout from a picture and so this can be loaded into Paintbrush as part of a larger Virtual image (ie a picture having more picture elements than can be shown on screen at once.

If at any time during either of these operations the computer beeps take note of the number of beeps. These are error messages from Frieze that will identify the problem but normally just check the printer or replace the disk and try again.

Emergency Procedures.

With the Olivetti Enhanced Graphics Boards or ATT DEB.

The Metawindows Graphics package uses the Display Enhancement Boards in a mode not specified by the BIOS. Unless the BIOS enhancement driver is used this means that when the BIOS tries to write send error messages to the screen it fails to map the characters correctly and so producing dark grey garbage on the screen. Unfortunately some programs (ie Pizzaz) are incompatible with this driver and the system will work better without it.

The most common cause is the message is "Device Not Ready Abort Retry Ignore" to which I recommend that you Abort by pressing the A key down once followed by a <Enter>. More garbage will appear then type <EGCMODE N> (Memoris: the mode change command for your specific adaptor if this is different) the standard DOS prompt should appear, then change directory back to D:\RAMD | otherwise REBOOT (CTRL-ALT-DEL). The normal causes of this error are; the printer is not switched on, the disk selected being full or the drive door open.

Filing and Sampling Errors.

The most common cause of this type of error is not enough RAM available to the Program. (Typically less than 128k when the program attempts to save, occurs when a lot of memory resident programs are in use and filing from **Inspect** or **View**). The solution is to remove all other RAM resident programs and then reload METAWNDO.

Screen Dumps on Dot Matrix Printers.

PrntScrn, Graphics, Pizzaz (PZ) or Frieze (Paintbush) should only be loaded if screen dumps are wanted. PrntScrn (supplied with Metawndows) works with most screens and Epson compatible dot matrix printers but only produces a medium resolution black and white plot. Graphics is part of DOS and normally only supports the IBM CGA adaptor on IBM printers but different machines may have other capabilities. (We use Olivetti machines and their version of Graphics supports 640x400 mono and 16 colour modes on colour and black Epson printers). We have successfully used all of these programs at different times. Other screen capture or printing programs that use Shift- PRT Scr as a hot key could be used but only one may be loaded at a time.

Pizzaz unfortunately can cause the filing problems above so the /s option should always be used.

WARNING ON MEMORY RESIDENT PROGRAMS.

If free memory is below 358,752 at start then file operations from inspect or View may not work properly. The critical value appears to be 128,000 bytes (<128k) free memory when the buffer is requested. These values were determined with an ATT DEB/Olivetti EGC board and does vary with different graphics cards. The free memory found is displayed on a pop up as a reminder of this. If you have problems please let me know the value and screen card/mode involved.

If lots of device drivers or memory resident programs are present then the program may fail with an error code of FF. This is a turbo Pascal error (Heap/Stack collision) and indicates insufficient memory.

Index

| | | | |
|------------------------------|------------|--------------------------------|--------|
| ADEVMR | 104 | plot files | 86 |
| Areas | 79, 87, 88 | Export files | 100 |
| Setting | 89 | File name | 86 |
| Setup | 82 | File Name | |
| ASCII export | 78 | Ending/type | 99 |
| AutoPoint | 103 | Export files | 86 |
| Averageing | 82 | File types | 99 |
| Averaging | 78 | Filing | 99 |
| Baud rate | 86 | FRIEZE | 106 |
| Bin Width | 96 | Hard copy | 78, 80 |
| Calibration | 87 | Epson | 80 |
| Channels | | HP plotter | 81 |
| Analog in (ADC) | 88 | IBM Printer | 80 |
| Analog out (DAC) | 88 | Image export | 78 |
| Colours | 86 | Input | |
| COM1 | 86 | Analog | 85 |
| Combining pointers | 103 | Channel 8 | 87 |
| CombPTr | 103 | Replay trigger | 88 |
| Current area | 79 | Sample trigger | 88 |
| Current channel | 87, 92 | Input range | 79 |
| Choose | 94 | Interleave | 91, 93 |
| Current section | 79 | KILL | 105 |
| length | 88 | LaserPlotter | 86 |
| Start | 88 | Loading the Program | 78 |
| Display type | 101 | ManPoint | 103 |
| Colour | 102 | Manual entry of pointers | 103 |
| Monochrome | 103 | MassRam | |
| setting | 78 | areas | 79 |
| Evenly spaced pointers | 103 | size | 79 |
| Export | | MRHOST | 105 |

| | |
|--------------------------|-------------|
| Number of channels | 79 |
| Output | |
| analog | 78 |
| Output Range | 79 |
| PaintLrush | 81, 86, 106 |
| Save image | 93 |
| Parity | 86 |
| Plotter setup | 85 |
| Pointers | 78, 80 |
| Clearing | 93 |
| File name | 95 |
| Loading | 96 |
| Printing | 96 |
| Saving | 96 |
| Select | 91 |
| Setting | 93 |
| Replay data | 81 |
| Replay rates | |
| Set | 88 |
| Replaying | |
| Continuous | 90 |
| Sample data | 81 |
| Sample rates | |
| Maximum | 83 |
| Sampling | 90 |
| Sampling rate | |
| Set | 88 |
| Sampling rates | |
| Maximum | 83 |
| Screen Dumps | 108 |
| Setup | 87 |
| Tramlines | 80 |
| Trigger mode | 88 |
| Units | |
| y axis | 88 |